Discovery of 3-((dimethylamino)methyl)-4-hydroxy-4-(3-methoxyphenyl)-N-phenylpiperidine-1-carboxamide as novel potent analgesic

Huoming Huang, Wenli Wang, Xuejun Xu, Chen Zhu, Yujun Wang, Jinggen Liu, Wei Li, Wei Fu

PII: S0223-5234(20)30037-4

DOI: https://doi.org/10.1016/j.ejmech.2020.112070

Reference: EJMECH 112070

To appear in: *European Journal of Medicinal Chemistry*

Received Date: 27 December 2019

Revised Date: 12 January 2020

Accepted Date: 13 January 2020

Please cite this article as: H. Huang, W. Wang, X. Xu, C. Zhu, Y. Wang, J. Liu, W. Li, W. Fu, Discovery of 3-((dimethylamino)methyl)-4-hydroxy-4-(3-methoxyphenyl)-N-phenylpiperidine-1-carboxamide as novel potent analgesic, *European Journal of Medicinal Chemistry* (2020), doi: https://doi.org/10.1016/j.ejmech.2020.112070.

Discovery of

3-((dimethylamino)methyl)-4-hydroxy-4-(3-methoxyphenyl)-N-phenylpiperidine-1-carboxamide as Novel Potent Analgesic

Huoming Huang [a], Wenli Wang [a], Xuejun Xu [b], Chen Zhu [a], Yujun Wang [b], Jinggen Liu [b*], Wei Li [a*], Wei Fu [a*]

Affiliation:

a. Department of Medicinal Chemistry, School of Pharmacy, Fudan University, Shanghai, 201203, China.

b. Shanghai Institute of Materia Medica, Chinese Academy of Science, Shanghai, 201203, China.

Graphical Abstract

2a

$K_{i\ MOR}$ = 7.3 ± 0.5 nM
$K_{i\ DOR}$ = 849.4 ± 96.6 nM
$K_{i\ KOR}$ = 49.1 ± 6.9 nM
ED_{50} = 3.1 mg/kg (hot plate model)
Antinociceptioin was blocked by naloxone

12

$K_{i\ MOR}$ = 1.2 ± 0.14 nM
$K_{i\ DOR}$ = 103.6 ± 0.9 nM
$K_{i\ KOR}$ = 71.38 ± 4.03 nM
$EC_{50\ MOR}$ = 2.3 ± 0.12 nM, E_{max} =240.0± 0.8%
$EC_{50\ DOR}$ = 112.2 ± 7.2 nM, E_{max} =254.1± 5.3%
$EC_{50\ KOR}$ = 110.4 ± 5.3 nM, E_{max} =196.6± 3.8%

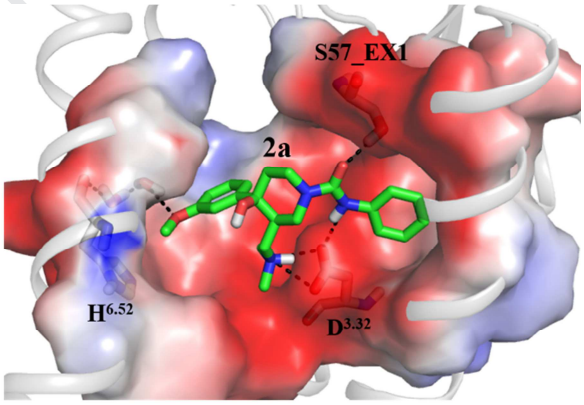

Discovery of

3-((dimethylamino)methyl)-4-hydroxy-4-(3-methoxyphenyl)-N-phenylpiperidine-1-carboxamide as Novel Potent Analgesic

Huoming Huang [a], Wenli Wang [a], Xuejun Xu [b], Chen Zhu [a], Yujun Wang [b], Jinggen Liu [b*], Wei Li [a*], Wei Fu [a*]

Affiliation:

a. Department of Medicinal Chemistry, School of Pharmacy, Fudan University, Shanghai, 201203, China.

b. Shanghai Institute of Materia Medica, Chinese Academy of Science, Shanghai, 201203, China.

Abstract:

Management of moderate to severe pain by clinically used opioid analgesics is associated with a plethora of side effects. Despite many efforts have been dedicated to reduce undesirable side effects, moderate progress has been made. In this work, starting from Tramadol, a series of 3-((dimethylamino)methyl)-4-hydroxy-4-(3-methoxyphenyl)piperidine-1-carboxamide derivatives were designed and synthesized, and their *in vitro* and *in vivo* activities were evaluated. Our campaign afforded selective μ opioid receptor (MOR) ligand **2a** ($K_{i\ MOR}$: 7.3±0.5 nM; $K_{i\ DOR}$: 849.4±96.6 nM; $K_{i\ KOR}$: 49.1±6.9 nM) as potent analgesic with ED_{50} of 3.1 mg/kg in 55^0C hot plate model. Its antinociception effect was blocked by opioid antagonist naloxone. High binding affinity toward MOR of compound **2a** was associated with water bridge, salt bridge, hydrogen bond and hydrophobic interaction with MOR. The high selectivity of compound **2a** for MOR over δ opioid receptor (DOR) and κ opioid receptor (KOR) was due to steric hindrance of compound **2a** with DOR and KOR. **2a**, a compound with novel scaffold, could serve as a lead for the development of novel opioid ligands.

Keywords: Selective MOR agonists; Antinociception; Analgesic; Opioids; Molecular mechanism

Introduction

Management of moderate to severe pain in clinics relied heavily on opioid analgesics due to their effectiveness in relieving pain. Clinically used opioids were divided into three categories, naturally derived morphinans such as Morphine, semi-synthetic morphinan analogues such as Oxycodone, Hydromorphone, and synthetic narcotic analgesics, such as Fentanyl, Tramadol and Pethidine (**Figure 1**)[1]. However, despite their desirable effectiveness in amelioration of pain, continued use of opioids was associated with a plethora of undesirable effects including, but not limited to, respiratory depress[2, 3], tolerance[4], dependence or abuse[5], constipation[6], nausea and vomiting[7]. In addition, overdose related mortality in America increased exponentially in recent years mainly due to prescription or illegal use of opioids[8-10]. Thus, analgesics with potent antinociception effect and without or with reduced side effects were in great demand in clinical practice. Many efforts have been devoted to the development of analgesics with reduced

undesirable effects, such as combination therapy of agonist and antagonist[11], new formulation strategy[12, 13]. These efforts led to moderate improvement.

Opioids elicited its analgesic effect via activating μ opioid receptor (MOR)[14, 15]. The opioid receptors belonged to G protein coupling receptor (GPCR) and generally were categorized into three subtypes: MOR, δ opioid receptor (DOR) and κ opioid receptor (KOR)[16]. Recently, it was found that G_i-biased MOR agonists that do not recruit β-arrestin 2 displayed improved antinociception effect and less side effects such as constipation, respiratory inhibition and tolerance[17-21]. The most advanced drug was biased MOR agonist TRV130 (**Figure 1**), which was not approved by FDA due to its safety concern[22-26], presumably its addiction liability[27]. In addition, it has been reported that G_i-biased KOR agonists were superior to balanced KOR agonists in antinociception and do not induce sedation and anhedonia-like actions[28, 29]. Several biased KOR agonists have been reported but none has entered clinical trial to date[30-36]. Many strategies targeting none opioid receptors such as ion channel, enzyme, for the management of moderate to severe pain, have been reported, but no new treatments were available in the market to date[37, 38].

As part of our continued interest in developing analgesics, Tramadol was selected as lead compound for its moderate side effects and pain-relieving effects. Recently, modification of Tramadol afforded selective MOR agonists and DOR agonists[39, 40]. Herein, we reported the design, synthesis, structure activity relationship and antinociception of 3-((dimethylamino)methyl)-4-hydroxy-4-(3-methoxyphenyl)-N-phenylpiperidine-1-carboxamide (**2a**). Also, binding pose of compound **2a** with MOR was proposed.

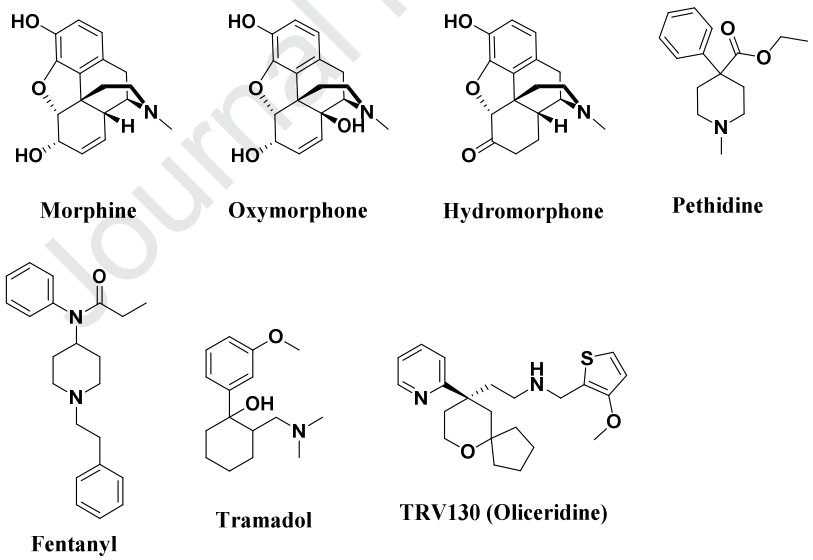

Figure 1 Structure of clinically used opioids and TRV130.

Compound design

Tramadol's moderate analgesic effect and metabolically labile property were associated with large oral dosing (100 mg) and relatively short duration (every 4~6 hours), respectively[41]. Furthermore, the maximum dose of tramadol was 400 mg per day, suggesting its potential relatively high toxicity[41]. "Message-address concept", proposed by Schwyzer in 1977[42], has been extensively used in the design of opioid ligands with varied selectivity over opioid receptors[43-46]. For example, the upper part of compound **1**, a balanced MOR/DOR ligand, corresponds to "message", while the bottom part belongs to "address" that determined its

selectivity (**Figure 2**)[47]. By carefully examining the structure of Tramadol, it was proposed that *meta*-methoxyphenyl and dimethylamine correspond to "message" part (**Figure 2**). Therefore, it would be interesting to probe where the "address" part of tramadol derivatives is and position 4 of cyclohexane ring of tramadol would be a good start. For the ease of synthesis, carbon atom of position 4 was replaced by nitrogen. Then phenyl was employed to probe the "address" part and urea group was selected as linker to add hydrogen donor and receptor with an aim to enhance its activity and hydrophilicity. As a result, compound **2a** was designed (**Figure 2**). To confirm our preliminary hypothesis, compound **2a** was docked into the active site of MOR and the binding mode was shown in **Figure 3A**. Compound **2a** fitted into the binding pocket of MOR well. Multiple interactions including water bridge, hydrogen bond and salt bridge interaction were observed for compound **2a**, suggesting that it would bind to MOR tightly and hence enhance its activity. In addition, **2a** aligned with Tramadol well and phenyl attaching to nitrogen extended into a hydrophobic pocket (**Figure 3B**). Based on above hypothesis and docking studies, nitrogen substitution patterns were explored and finally compound **2a**~**2r** were designed (**Figure 2**).

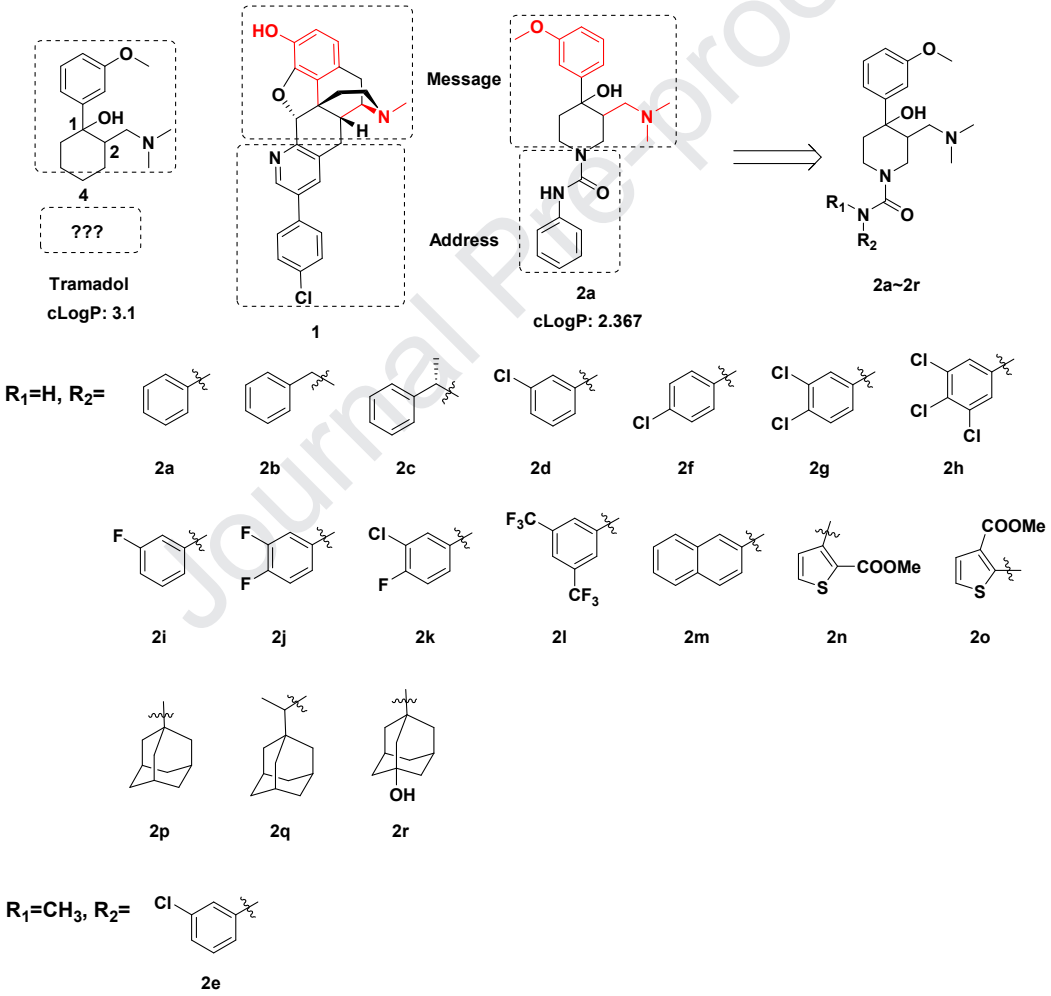

Figure 2 Design of target compounds

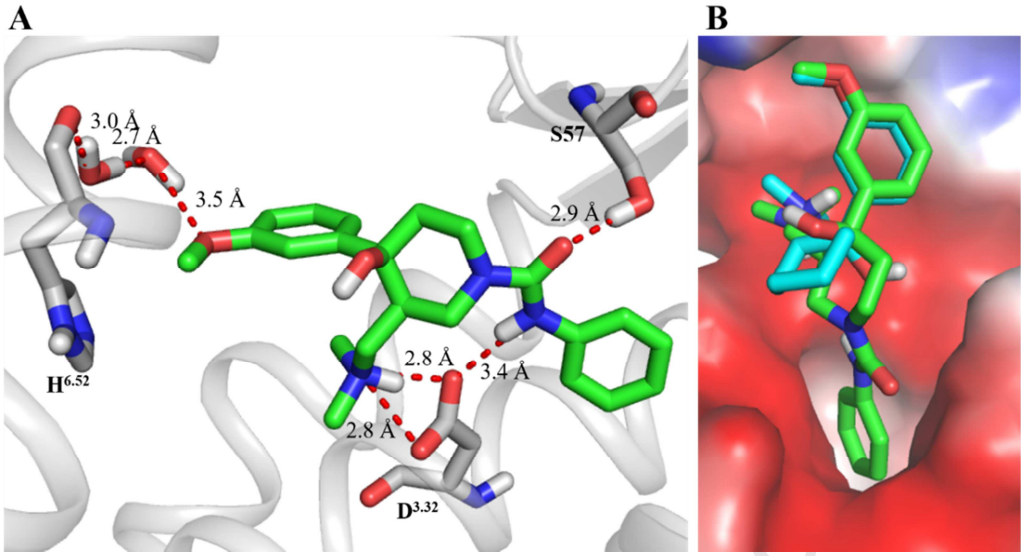

Figure 3 Binding mode of **2a** with MOR and alignment of Tramadol with **2a**. (**A**: Binding mode of **2a** with MOR. **2a** was shown in sticks, green. **B**: Alignment of Tramadol with **2a**. Tramadol was shown in sticks, light blue.)

Chemistry

Synthesis of target compounds were shown in **Figure 4**, **Figure 5** and **Figure 6**. Initially, synthetic route shown in **Figure 4** was employed. Hydroxyl in compound **3** was protected by triethylsilyl (TES) using triethylchlorosilane (TESCl) in the presence of imidazole to afford **4**, which reacted with isocyanate **5** to give **6**. Compound **6** was deprotected in tetrabutylammonium fluoride (TBAF) to give free base, which underwent salt formation to get hydrochloride **2d**. However, several disadvantages were obvious. Protecting group TES was not stable, making **4** undergo deprotection at room temperature. Isocyanates are highly toxic and many are not commercially available. Therefore, synthetic route in **Figure 5** was devised and implemented. Phenyl chloroformate or *para*-nitrophenyl chloroformate reacted with amines to give **8**[48], followed by reaction with **3** to obtain **9**. Free base **9** reacted with HCl to give **2a**~**2c**, **2e**~2**r**. Compound **12** reacted with phenyl phenylcarbamate to give **11** as free base, which underwent salt formation with HCl to give **12** (**Figure 6**). All final compounds were confirmed by ^{1}H NMR, ^{13}C NMR and HRMS.

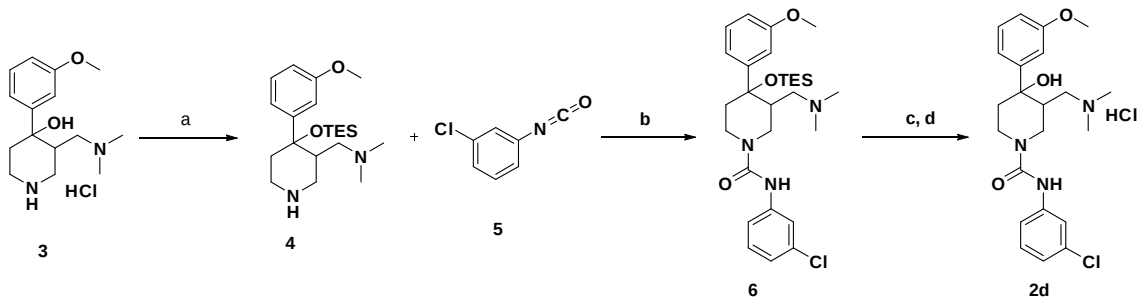

Figure 4 Initial synthesis of compound **2d**. (a) TESCl, imidazole, DCM; b) TEA, DCM, 0^{0}C~R.T.; c) TBAF, THF, R.T. d) HCl/Dioxane.)

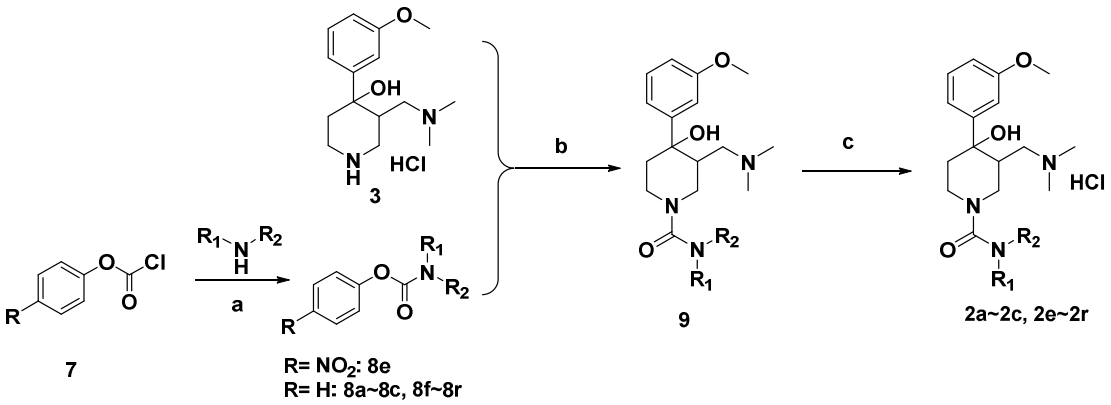

Figure 5 Modified route for the synthesis of compound **2a**~**2c**, **2e**~**2r**. (a) $NaHCO_3$, THF/H_2O, R.T.; b) TEA, DMF, R.T.; c) HCl/Dioxane.)

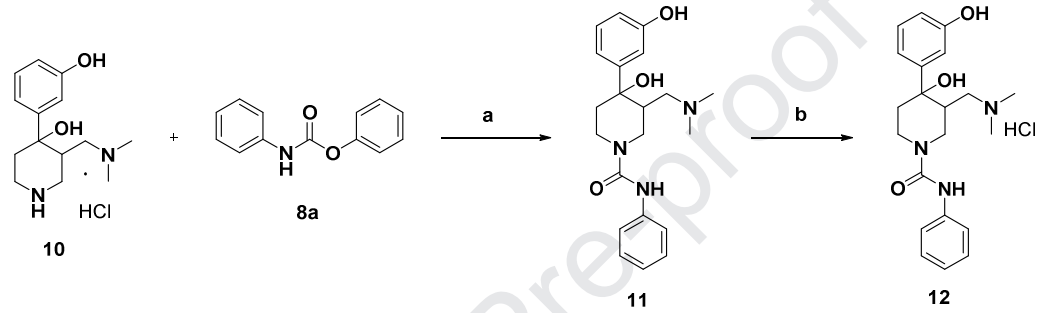

Figure 6 Synthesis of **12** (a) TEA, DCM, R.T.; b) HCl/Dioxane, R.T.)

Results and Discussion

55 ^{0}C hot plate model is a reliable animal model extensively used in the evaluation of compounds acting on pain perception via central nervous systems[49]. It's readily available in our lab. Therefore, we employed a combination strategy of *in vitro* binding affinity and *in vivo* 55 ^{0}C hot plate model screening simultaneously. Evaluation on animal model was first tested at dosage 10 mg/kg via intraperitoneal injection. Compounds that displayed full antinociception (Maximum possible effect% (MPE%) was 100%) was further studied in detail. Compounds that showed partial antinociception (defined as MPE% <100%) at 10 mg/kg will not investigate further.

Binding affinities of target compounds were evaluated in radioligand binding assay and summarized in **Table 1**. Tramadol showed weak binding affinities for three opioid receptors and is in consistent with literature[50]. Compound **2a** with phenyl ring attached to nitrogen displayed high affinity (K_i = 7.3 ± 0.5 nM) and selectivity for MOR over DOR and KOR. Its high binding for MOR further confirmed our hypothesis. Compound **2a** displayed full antinociception at dose of 10 mg/kg in hot plate model. Substitution of phenyl with benzyl group afforded **2b**, which showed sharply decreased binding for three receptors. This indicated that benzyl with higher flexibility and longer chain was incompatible with three receptors in the sub-pocket. Adding methyl to the metabolically labile benzyl position gave **2c**. Compound **2c** also showed lower binding for MOR as well as KOR in compare with **2b** and abolished affinity for DOR. Compound **2b** and **2c** showed partial antinociception *in vivo*.

We next turn our attention to explore substitution patterns on phenyl ring. *Meta*-chloro bearing **2d** displayed one-fold decrease in affinity for MOR and 15-fold decrease for KOR, but increase for DOR in comparison to **2a**. Also, compound **2d** was a selective ligand for MOR. Deleting hydrogen bond donor in **2d** by adding methyl group yielded **2e**. Compound **2e** showed

substantially decreased binding for three opioid receptors, suggesting hydrogen bonding was favorable in this position. Moving *meta*-chloro to *para* position (**2f**), or multi-substitution in phenyl (**2g** and **2h**) decreased their binding for MOR and KOR greatly in comparison to **2d**, and abolished affinity for DOR. Compound **2d**~**2h** showed partial antinociception *in vivo*. Substitution of *meta*-chloro with fluoro lead to **2i**. Compound **2i** showed decreased binding for MOR and DOR as well as abolished activity for KOR. However, **2i** showed potent antinociception *in vivo*. In consistent with **2g** and **2h**, multi-substitution **2j** and **2k** showed low binding for three opioid receptors. *Meta*-bis(trifluoromethyl) and β-naphthyl substitution gave **2l** and **2m**, respectively. Compound **2l** and **2m** showed abolished activities for MOR and low binding for DOR and KOR. Adding hydrogen bond acceptor ester group to thienyl (**2o** and **2p**) displayed no improvement in affinities for three receptors.

It has been reported that binding pockets of opioid receptors were exposed to extracellular side[51-54]. The nitrogen substitution corresponded to the "address" part (**Figure 2**). We next explored the "address" pocket by adding bulky adamantyl and gave **2p**, **2q** and **2r**. Unfortunately, it turned out that **2p**~**2r** showed decreased or abolished binding for opioid receptors, indicating that adamantyl is too bulky for these receptors. Overall, **2j**~**2r** showed partial antinociception *in vivo*.

Table 1 Binding affinities of compound **2a**~**2r**

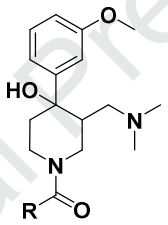

Compounds	R	K_i (nM) or Inhibition at 1 μM (%) [a]			*In vivo* activity [e]
		MOR [b]	DOR [c]	KOR [d]	
Tramadol	--	6.0±0.4%	0%	0%	--
DAMGO	--	2.30±0.02	ND [f]	ND	--
DPDPE	--	ND	2.30±0.69	ND	--
U50488	--	ND	ND	0.91±0.20	--
2a		7.3±0.5	849.4±96.6	49.1±6.9	100%
2b	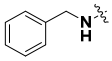	35.1±4.4%	2.6±2.9%	5.1±4.0%	partial
2c	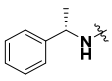	20.5±5.5%	0%	4.1±6.7%	partial
2d	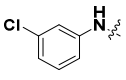	14.1±2.7	537±69.3	718.6±197.0	partial
2e	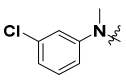	8.7±3.7%	0%	14.0±9.7%	partial
2f	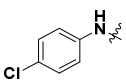	48.8±3.9%	0%	22.1±10.7%	partial

2g	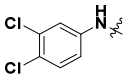	46.0±5.4%	0%	18.2±1.9%	partial
2h	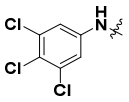	13.2±8.0%	0%	0%	partial
2i	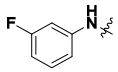	36.7±7.4%	9.2±7.8%	0%	100%
2j	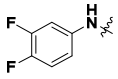	13.6±13.1%	16.4±10.6%	0%	partial
2k	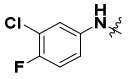	25.0±13.3%	21.6±13.4%	7.1±5.0%	partial
2l	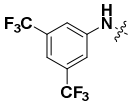	0%	0.9%	8.6±4.8%	partial
2m	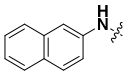	0.5%	0%	3.9%	partial
2n	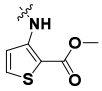	10.2±9.0%	0%	0%	partial
2o	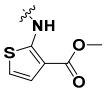	2.3%	16.0±12.4%	9.2±3.1%	partial
2p		13.5±4.8%	0%	17.9±4.8%	partial
2q		32.8±5.5%	0%	10.4±10.2%	partial
2r		0%	1.9%	0%	partial

a. Values are expressed as the mean ± SEM for three independent experiments performed in triplicate. b. Displacement of [^{3}H] DAMGO from the CHO cell membrane expressing the μ opioid receptor. c. Displacement of [^{3}H] DPDPE from the CHO cell membrane expressing the δ opioid receptor. D. Displacement of [^{3}H] U69593 from the CHO cell membrane expressing the κ opioid receptor. e. 55 ^{0}C hot plate model, i.p., mice, n=4~5. f. Not determined.

Compounds **2a** and **2i** were potent in 55 ^{0}C hot plate model at 10 mg/kg dose after intraperitoneal injection (**Table 1**). Lowering dose to 5 mg/kg, **2a** was more potent than **2i** (**Figure 7**). In addition, compound **2a** produced longer duration action than **2i** in this model. Therefore, **2a** was selected as candidate for further study. Compound **2a** dose dependently prolonged latency of mice to noxious stimuli in 55 ^{0}C hot plate model (**Figure 8**), and ED_{50} was determined as 3.1 mg/kg. In contrast, Tramadol showed partial antinociception activity up to 50 mg/kg. Furthermore, analgesic effect of compound **2a** was blocked by nonselective opioid antagonist naloxone (**Figure 9**). Taken high selectivity of compound **2a** for MOR and its antagonism effect by naloxone together, we assumed that **2a** produced its antinociception mainly via MOR.

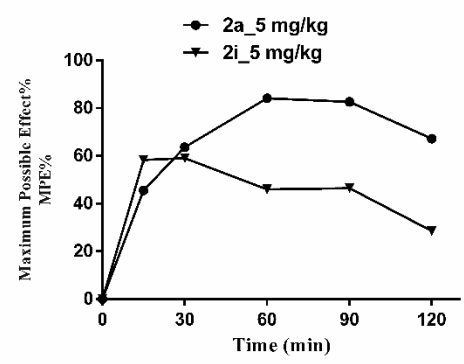

Figure 7 Comparison of antinociception of **2a** and **2i** at 5 mg/kg. (55□ hot plate model, mice, i.p., n=4)

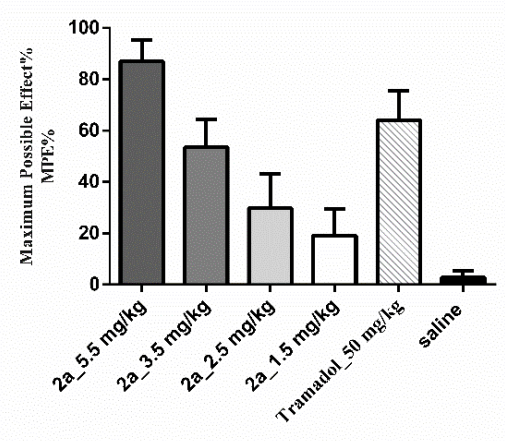

Figure 8 Antinociception of **2a** (55^0C hot plate model, mice, i.p., n= 9~14; shown was 60 min for **2a** and 15 min for tramadol.)

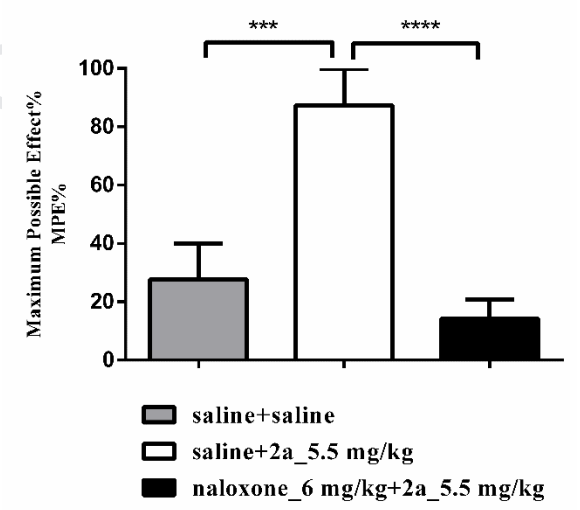

Figure 9 Antinociception of **2a** was antagonized by naloxone. Naloxone was injected intraperitoneally 10 min before dosing of **2a**. (55^0C hot plate, mice, i.p., n=7~8; p<0.0001: ****; p<0.001: ***)

Tramadol acted as a prodrug and its active metabolite is *O*-demethyl product **M1**[50, 55, 56]. As tramadol does, though **2a** binds to MOR tightly (K_i = 7.3±0.5 nM), the *O*-demethyl product of **2a** might be active to MOR. To verify it, its *O*-demethyl metabolite **12** was synthesized and its *in*

vitro activities were evaluated. As shown in **Table 2**, compound **12** showed high binding affinity and selectivity for MOR ($K_{i\,MOR}$: 1.2±0.14 nM) and its activity for MOR was ten-fold potent than that of **M1**. In addition, compound **12** showed seven-fold potent in binding activity for MOR than compound **2a** (**Table 1**). Also, compound **12** showed high potency for MOR and moderate potency for DOR and KOR, rendering it to be a selective MOR agonist (**Table 3**). These *in vitro* data gave us hint that **2a** may elicits its *in vivo* antinociception via both **2a** and **12**.

Table 2 Binding affinities of compound **12** for three opioid receptors

Compounds	Inhibition at 1 μM (%) or K_i (nM) [a]			DOR/MOR	KOR/MOR
	MOR [b]	DOR [c]	KOR [d]		
Tramadol	6.0±0.4%	0%	0%	--	--
M1	13.0±0.5	19.0±2.3%	20.2±0.1%	--	--
12	1.2±0.14	103.60±0.90	71.38±4.03	86.3	59.5

a. Values are expressed as the mean ± SEM for three independent experiments performed in triplicate. b. Displacement of [^{3}H] DAMGO from the CHO cell membrane expressing the μ opioid receptor. c. Displacement of [^{3}H] DPDPE from the CHO cell membrane expressing the δ opioid receptor. D. Displacement of [^{3}H] U69593 from the CHO cell membrane expressing the κ opioid receptor.

Table 3 Functional activity in stimulating [^{35}S] GTPγS binding of compound **12**

Compounds	[S^{35}] GTPγS assay					
	MOR		DOR		KOR	
	EC_{50} (nM) [a]	E_{max} (%)	EC_{50} (nM)	E_{max} (%)	EC_{50} (nM)	E_{max} (%)
M1	244.7 nM	225.7%	ND [b]	ND	ND	ND
DAMGO	8.06±0.75	205.0±2.05	ND	ND	ND	ND
DPDPE	ND	ND	1.43±0.15	231.3±7.05	ND	ND
U50488	ND	ND	ND	ND	2.77±0.08	199.5±6.30
12	2.3±0.12	240.0±0.8	112.2±7.2	254.1±5.3	110.4±5.3	196.6±3.8

a. Potency and efficacy in stimulating [^{35}S] GTPγS binding to CHO cell membranes stably expressing opioid receptors. Data are expressed as the mean ± SEM of independent experiments performed in triplicate. b. Not determined due to low stimulation.

Binding modes and selectivity of 2a on MOR

As shown in **Table 1**, compound **2a** showed high binding affinity and selectivity for MOR over DOR and KOR ($K_{i\,MOR}$: 7.3±0.5 nM; $K_{i\,DOR}$: 849.4±96.6 nM; $K_{i\,KOR}$: 49.1±6.9 nM). We next investigated the intrinsic reasons of its high binding and selectivity. Engagement of $H^{6.52}$ and $D^{3.32}$ has been reported to be involved in the activation process of MOR. As shown in **Figure 3A**, in consistent with morphine and its derivative, where the phenol hydroxyl engaged in hydrogen bonding with $H^{6.52}$ via two water molecules, oxygen of methoxy group interacted with $H^{6.52}$. Protonated nitrogen of dimethylamine participated in salt bridge interaction with $D^{3.32}$. As suggested in structure activity relationship exploration, NH in urea group also engaged in the interaction with $D^{3.32}$ via hydrogen bonding, highlighting its importance for its high binding affinity. Carbonyl oxygen in urea group hydrogen bonded with S57. Phenyl attaching to nitrogen extended into the hydrophobic pocket flanked by $Val^{3.28}$, $Gln^{3.09}$, $Thr^{3.04}$, $Phe^{3.08}$ and $Trp^{3.18}$ (**Figure 10A**). All these forces contributed to its high binding for MOR. To further explain the selectivity of **2a** to MOR over KOR and DOR, the sequences alignment in binding site of MOR with DOR and KOR were conducted. As shown in **Figure 10E**, three residues in positions 3.11,

7.15 and 7.35 among three opioid receptors are different and thus makes the shapes and electrostatic potential of active sites different (**Figure 10C** and **10D**), leading to different pharmacological profile of **2a** in three opioid receptor subtypes. It underlies the high selectivity of **2a** for MOR over KOR and DOR.

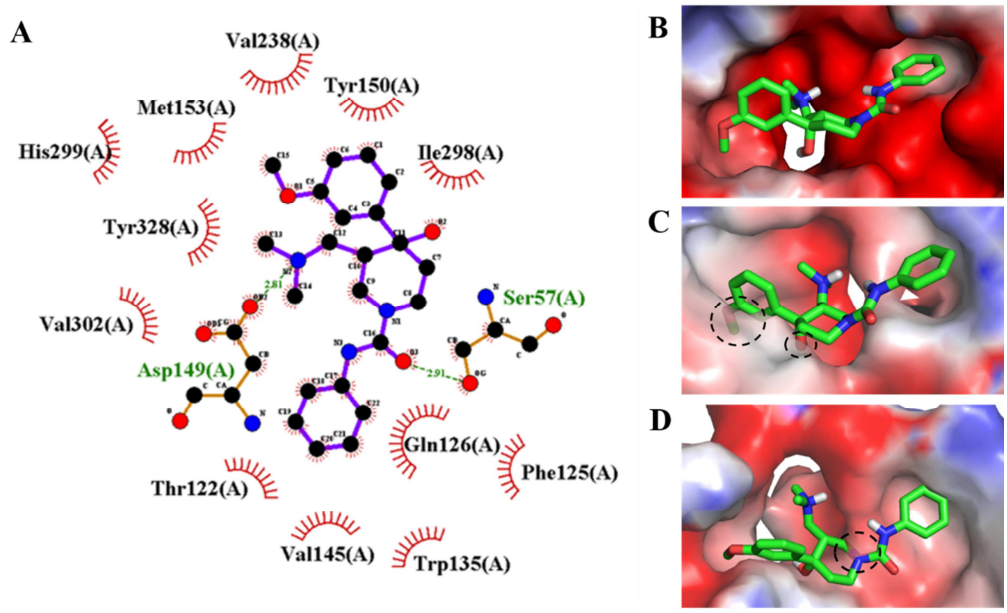

E

	ECL1	ECL1	3.05	3.08	3.09	3.11	3.18	3.28	3.29	3.32	3.33	3.36	5.39	5.42	6.48	6.51	6.52	7.17	7.35	7.39	7.43
MOR	D	S	T	F	Q	N	W	V	I	D	Y	M	K	V	W	I	H	V	W	I	Y
DOR	--	--	T	F	Q	K	W	V	I	D	Y	M	K	V	W	I	H	V	L	I	Y
KOR	--	--	T	F	Q	V	W	V	I	D	Y	M	K	V	W	I	H	I	Y	I	Y

Figure 10 Binding modes of compound **2a** with opioid receptors. (**A**: Dimensional diagram of **2a** with MOR. **B**: Electrostatic potential map of **2a** with MOR. **2a** was shown in sticks, green. **C**: Electrostatic potential map of **2a** with DOR. **D**: Electrostatic potential map of **2a** with KOR. **E**: The sequences alignment in active binding site of MOR with KOR and DOR.)

Conclusion

In summary, using Tramadol as a lead compound, a series of 3-((dimethylamino)methyl)-4-hydroxy-4-(3-methoxyphenyl)-N-phenylpiperidine-1-carboxamide derivatives were designed, synthesized and their activities were evaluated *in vitro* and *in vivo*. Furthermore, the structure activity relationship was extensively explored. *In vitro* and *in vivo* screening afforded highly selective MOR ligand **2a** ($K_{i\ MOR}$: 7.3±0.5 nM; $K_{i\ DOR}$: 849.4±96.6 nM; $K_{i\ KOR}$: 49.1±6.9 nM) as potent analgesic in 55 ^{0}C hot plate model in mice and ED_{50} was 3.1 mg/kg. Its antinociception was antagonized by nonselective antagonist naloxone. Water bridge, salt bridge, hydrogen bond and hydrophobic interaction with MOR contributed to compound **2a**'s high affinity for MOR. After alignment of sequences at binding sites of three opioid receptors, steric hindrance of **2a** with DOR and KOR explained its high selectivity for MOR. Due to its potent *in vivo* analgesic effect, as well as ease of synthesis in comparison to naturally-derived morphinans, compound **2a** could serve as a novel scaffold for the development of novel opioid ligands that might combat morphine-like side effects.

Experimental section

General aspects

All chemicals and solvents were supplied by Tansoole or Adamas or other suppliers and were used without further purification. ^{1}HNMR and ^{1}CNMR spectra were recorded on Varian-400 instrument, Bruker-600 MHz instrument, respectively. Proton coupling patterns were described as singlet, doublet, triplet, quartet, multiple, and broad. Mass spectra were generated with electric spray ionization (ESI) produced by an analytical Agilent 1200 liquid chromatography-mass spectrometer tandem instrument. High-resolution mass spectrometry (HRMS) spectra were recorded with an AB 5600+ Q TOF instrument.

Chemical synthesis

1-(4-(3-methoxyphenyl)-4-((triethylsilyl)oxy)piperidin-3-yl)-N,N-dimethylmethanamine (4)

To a 250 ml three neck flask equipped with nitrogen gas balloon, constant pressure dropping funnel and thermometer was charged with **3** (10 g, 33.22 mmol, 1 eq.), imidazole (20.35 g, 298.98 mmol, 9 eq.), DCM (100 ml). The resulting clear solution was cooled with ice water bath and triethylchlorosilane (35.06 g, 232.6 mmol, 7 eq.) was added under 10^{o}C. After the addition, the coolant was removed and the mixture was stirred overnight. Reaction mixture was added slowly to sodium bicarbonate solution (100 ml) and stirred for 10 min. Then the aqueous phase was extracted with DCM three times (75+25+25 ml). The combined organic layers were washed with water (20 ml), dried over anhydrous magnesium sulfate, filtered and evaporated under reduced pressure to give 36.7 g yellow oil, which was subjected to Al_2O_3 fast column chromatography to yield 10.2 g pale yellow oil and used without further purification. LC-MS: ESI^{+} $[M + H]^{+}$ 379.1.

N-(3-chlorophenyl)-3-((dimethylamino)methyl)-4-(3-methoxyphenyl)-4-((triethylsilyl)oxy)piperidine-1-carboxamide (6)

To a 50 ml three neck flask equipped with nitrogen gas balloon, constant pressure dropping funnel and thermometer was added with **4** (0.6 g, 1.59 mmol, 1 eq.), DCM (6 ml), TEA (0.193 g, 1.91 mmol, 1.2 eq.). The mixture was cooled to -5^{0}C and a solution of 1-chloro-3-isocyanatobenzene (**5**, 0.244 g, 1.59 mmol, 1 eq.) in DCM (2 ml) was added dropwise under 0^{0}C. The reaction mixture was stirred for 3 h. After the completion of reaction, water (25 ml) and DCM (10 ml) were added. The organic layer was separated by funnel. Then the aqueous phase was extracted with DCM (15 ml). The organic layers were combined, washed with water (10 ml) and evaporated under reduced pressure to give 1.1 g pale yellow oil, which underwent fast column chromatography to afford 0.8 g pale yellow oil and used without further purification.

N-(3-chlorophenyl)-3-((dimethylamino)methyl)-4-hydroxy-4-(3-methoxyphenyl)piperidine-1-carboxamide hydrochloride (2d)

To a 50 ml flask was added **6** (0.75 g, 1.41 mmol, 1 eq.), THF (8 ml) and TBAF-3H_2O (0.67 g, 2.114 mmol, 1.5 eq.). The mixture was stirred at room temperature overnight. The reaction was monitored by TLC (DCM: MeOH = 15:1, v/v). After the reaction, the THF was removed by evaporation under reduced pressure and $NaHCO_3$ solution (30 ml) was added. The aqueous phase was extracted with DCM (15+15 ml). The combined organic layers were washed with water (20 ml), dried over $MgSO_4$, filtered and evaporated under reduced pressure to give 0.8 g residue, which was purified by column chromatography to give 0.66 g off-white solid. The resulting solid was recrystallized in IPA: EA: PE (0.5 ml: 0.5 ml: 2.5 ml) to obtain 0.47 g off-white solid. Then 0.35 g off-white solid, DCM (3.5 ml) and Methanol (0.5 ml) were added to 50 ml flask. To the clear solution was added HCl/dioxane (0.25 ml, 1.008 mmol, 1.2 eq.) and then MTBE (5 ml) was added dropwise. After stirring for 4 hours, 0.31 g off-white solid was collected by filtration (yield 64%). ^{1}H NMR (400 MHz, CD_3OD), δ 7.64~7.65 (m, 1H), 7.37~7.39 (m, 1H), 7.33 (t, J = 8 Hz,

1H), 7.22~7.26 (t, 1H), 7.4~7.15 (m, 1H), 7.09 (d, *J* = 4 Hz, 1H), 7.01 (dd, *J* = 8 Hz, *J* = 4 Hz, 1H), 6.86 (dd, *J* = 8 Hz, *J* = 4 Hz, 1H), 4.43~4.68 (m, 1H), 4.08~4.12 (m, 1H), 3.81 (s, 3H), 3.38~3.45 (m, 1H), 3.24~3.34 (m, 1H), 3.01~3.06 (m, 1H), 2.72~2.75 (m, 4H), 2.57 (s, 3H), 2.38~2.44 (m, 1H), 2.17~2.25 (m, 1H), 1.71~1.76 (m, 1H). ^{13}C NMR (150 MHz, CD_3OD) δ 159.50, 155.24, 146.62, 140.56, 133.13, 128.86, 128.76, 121.67, 119.48, 117.71, 116.39, 111.47, 110.50, 72.41, 56.62, 53.68, 42.90, 40.53, 39.93, 38.49. LC-MS-ESI+: $[M + H]^+$ 418.2. HRMS (ESI), calcd for $C_{22}H_{28}ClN_3O_3$ $[M + H]^+$, 418.1892; found, 418.1888.

General procedure for the synthesis of 8

Take the synthesis of phenyl naphthalen-2-ylcarbamate (**8m**) as example

To a 100 ml three neck flask equipped with thermometer was added naphthalen-2-amine (2 g, 13.97 mmol, 1 eq.), THF (20 ml), $NaHCO_3$ (1.41 g, 14.67 mmol, 1.2 eq.) and cooled to 0^0C. Then a solution of phenyl chloroformate (1.84 g, 14.67 mmol, 1.05 eq.) in THF (10 ml) was added dropwise under 5^0C. The reaction was monitored by TLC. After completion of the reaction, THF was removed by evaporation under reduced pressure. The aqueous phase was extracted with ethyl acetate (50+25 ml). The combined organic layers were washed with brine (20 ml), dried over anhydrous magnesium sulfate, filtered and evaporated under reduced pressure to give 3.5 g brown solid, which was subjected to crystallization in EA:PE (1:2 / v:v, 45 ml) to give 3 g off-white solid (yield 81.5%). ^{1}H NMR (400 MHz, $CDCl_3$), δ 8.07 (s, 1H), 7.76~7.86 (m, 3H), 7.39~7.50 (m, 5H), 7.22~7.29 (m, 3H), 7.13 (m, 1H). LC-MS-ESI$^+$: $[M + H]^+$ 264.1, $[M + Na]^+$ 286.1.

General procedure for the synthesis of 2 and 12

Take the synthesis of 3-((dimethylamino)methyl)-4-hydroxy-4-(3-methoxyphenyl)-N-(naphthalen-2-yl)piperidine-1-carboxamide hydrochloride (**2m**) as example.

To a 100 ml flask was added **3** (0.6 g, 2 mmol,1 eq.), DCM (10 ml), TEA (0.71 g, 7 mmol, 3.5 eq.) and the resulting mixture was stirred till the completion of reaction. Water (30 ml) was added and extracted with DCM (10+10 ml). Organic layers were combined, washed with water (10 ml), dried over anhydrous magnesium sulfate, filtered and evaporated under reduced pressure to give 0.72 g brown oil. The free base was purified by silica gel column chromatography to obtain 0.45 g foam (yield 51%). To a 100 ml flask was added the free base (.4 g, 0.923 mmol, 1 eq.), DCM (3 ml), MeOH (1 ml) and to the resulting clear solution was added HCl/dioxane (0.35 ml, 1.384 mmol, 1.5 eq.). Then MTBE (20 ml) was added dropwise. After stirring for 3 hours, the solid was filtered, dried under reduced pressure to 0.38 g off-white soli (87.6%). ^{1}H NMR (400 MHz, CD_3OD), δ 7.83 (s, 1H), 7.59~7.65 (m, 3H), 7.47~7.51 (m, 1H), 7.26~7.30 (m, 1H), 7.17~7.23 (m, 2H), 6.94~7.02 (m, 1H), 6.73 (d, *J* = 8 Hz, 1H), 4.36 (d, *J* = 12 Hz, 1H), 4.03 (d, *J* = 12 Hz, 1H), 3.68 (s, 3H), 3.29~3.36 (m, 1H), 3.06~3.21 (m, 1H), 2.92 (t, *J* = 12 Hz, 1H), 2.51~2.63 (m, 7H), 2.30 (m, 1H), 2.08~2.16 (m, 1H), 1.63 (d, *J* = 8 Hz, 1H). ^{13}C NMR (150 MHz, CD_3OD) δ 159.51, 155.80, 146.69, 136.52, 133.35, 129.64, 128.87, 127.15, 126.50, 126.19, 125.22, 123.51, 120.64, 116.41, 116.02, 111.47, 110.53, 72.46, 56.66, 53.69, 43.08, 40.60, 39.93, 38.52. LC-MS-ESI$^+$: $[M + H]^+$ 434.3. LC-MS-ESI$^-$: $[M + H]^-$ 432.4, $[M + Cl^-]^-$ 468.3. HRMS (ESI), calcd for $C_{26}H_{31}N_3O_3$ $[M + H]^+$, 434.2438; found, 434.2437.

3-((dimethylamino)methyl)-4-hydroxy-4-(3-methoxyphenyl)-N-phenylpiperidine-1-carboxamide hydrochloride (**2a**)

Phenyl phenylcarbamate (**8a**)

Off-white solid, yield: 95.2%. ^{1}H NMR (400 MHz, DMSO-d6), δ 10.26 (s, 1H), 7.52 (d, *J* = 8 Hz, 2H), 7.43 (t, *J* = 8 Hz, 2H), 7.33 (t, *J* = 8 Hz, 2H), 7.22~7.28 (m, 3H), 7.05 (d, *J* = 8 Hz, 1H).

3-((dimethylamino)methyl)-4-hydroxy-4-(3-methoxyphenyl)-N-phenylpiperidine-1-carboxamide hydrochloride (**2a**)

Off-white solid, yield: 81.4%. ^{1}H NMR (400 MHz, CD_3OD), δ 7.44~7.47 (m, 2H), 7.25~7.35 (m, 3H), 7.01~7.15 (m, 2H), 6.68~6.88 (m, 1H), 4.43~4.48 (m, 1H), 4.09~4.14 (m, 1H), 3.81 (s, 3H), 3.37~3.45 (m, 1H), 3.20~3.30 (m, 1H), 3.00~3.06 (m, 1H), 2.65~2.75 (m, 7H), 2.37~2.44 (m, 1H), 2.18~2.26 (m, 1H), 1.72~1.76 (m, 1H). ^{13}C NMR (150 MHz, CD_3OD) δ 159.49, 155.76, 146.69, 138.84, 128.85, 127.56, 122.20, 120.20, 116.39, 111.46, 110.51, 72.45, 56.66, 53.69, 43.00, 40.57, 39.86, 38.49. LC-MS-ESI$^+$: $[M + H]^+$ 384.3. HRMS (ESI), calcd for $C_{22}H_{29}N_3O_3$ $[M + H]^+$, 384.2282; found, 384.2282.

N-benzyl-3-((dimethylamino)methyl)-4-hydroxy-4-(3-methoxyphenyl)piperidine-1-carboxamide hydrochloride (**2b**)

Phenyl benzylcarbamate (**8b**)

Off-white solid, yield: 92%. ^{1}H NMR (400 MHz, $CDCl_3$), δ 7.31~7.41 (m, 7H), 7.11~7.26 (m, 3H), 5.37 (s, 1H), 4.44~4.51 (m, 2H). LC-MS-ESI$^+$: $[M + H]^+$ 227.1, $[M + Na]^+$ 250.1, $[2M + Na]^+$ 477.2.

N-benzyl-3-((dimethylamino)methyl)-4-hydroxy-4-(3-methoxyphenyl)piperidine-1-carboxamide hydrochloride (**2b**)

Off-white solid, yield: 83.5%. ^{1}H NMR (400 MHz, CD_3OD), δ 7.15~7.21 (m, 5H), 7.07~7.10 (m, 1H), 6.95 (d, *J* = 4 Hz, 1H), 6.87 (d, *J* = 8 Hz, 1H), 6.71 (d, *J* = 8 Hz, 1H), 4.26 (q, 2H), 4.13 (dd, *J1* = 12 Hz, *J2* = 4 Hz, 1H), 3.78 (d, *J* = 8 Hz, 1H), 3.66 (s, 3H), 3.15~3.25 (m, 1H), 3.03 (t, *J* = 12 Hz, 1H), 2.82~2.89 (m, 1H), 2.48~2.56 (m, 7H), 2.12~2.15 (m, 1H), 1.99 (m, *J1* = 16 Hz, *J2* = 4 Hz, 1H), 1.52~1.56 (m, 1H). ^{13}C NMR (150 MHz, CD_3OD) δ 159.48, 157.95, 146.69, 139.56, 128.84, 127.37, 126.33, 125.90, 116.32, 111.40, 110.50, 72.43, 56.60, 53.69, 43.28, 42.94, 40.40, 39.70, 38.28. LC-MS-ESI$^+$: $[M + H]^+$ 398.3. HRMS (ESI), calcd for $C_{23}H_{31}N_3O_3$ $[M + H]^+$, 398.2438; found, 398.2435.

3-((dimethylamino)methyl)-4-hydroxy-4-(3-methoxyphenyl)-N-((*S*)-1-phenylethyl)piperidine-1-carboxamide hydrochloride (**2c**)

Phenyl (*S*)-(1-phenylethyl)carbamate (**8c**)

Off-white solid, yield: 94%. ^{1}H NMR (400 MHz, $CDCl_3$), δ 7.26~7.41 (m, 7H), 6.97~7.21 (m, 3H), 5.34 (s, 1H), 4.89~4.97 (m, 1H), 1.55~1.60 (m, 3H). LC-MS-ESI$^+$: $[M + H]^+$ 242.2, $[M + Na]^+$ 264.2, $[2M + Na]^+$ 505.3.

3-((dimethylamino)methyl)-4-hydroxy-4-(3-methoxyphenyl)-N-((*S*)-1-phenylethyl)piperidine-1-carboxamide hydrochloride (**2c**)

Off-white solid, yield: 83.3%. ^{1}H NMR (400 MHz, CD_3OD), δ 7.22~7.24(m, 2H), 7.13~7.18(m, 3H), 7.05(s, 1H), 6.93(d, *J* = 12 Hz, 1H), 6.85(dd, *J1* = 16 Hz, *J2* = 4 Hz, 1H), 6.68~6.70(m, 1H), 4.75~4.81(m, 1H), 4.14(d, *J* = 16 Hz, 1H), 3.83(d, *J* = 16 Hz, 1H), 3.65(s, 3H), 3.14~3.17(m, 1H), 2.95~3.04(m, 1H), 3.83(t, *J* = 12 Hz, 1H), 2.50~2.58(m, 4H), 2.36~2.38(d, 3H), 1.94~2.10(m, 2H), 1.53(d, *J* = 16 Hz, 1H), 1.33~1.38(m, 3H). ^{13}C NMR (150 MHz, CD_3OD) δ 159.47, 157.31, 157.23, 146.74, 144.86, 144.78, 128.82, 127.39, 127.34, 125.75, 125.72, 125.12, 125.02, 116.35, 116.32, 111.41, 110.49, 110.46, 72.40, 56.62, 53.68, 49.96, 49.94, 43.04, 40.42, 40.37, 39.66, 39.58, 38.46, 38.23, 21.18, 21.05. LC-MS-ESI$^+$: $[M + H]^+$ 412.3. LC-MS-ESI$^-$: $[M + Cl^-]^-$ 446.2. HRMS (ESI), calcd for $C_{24}H_{33}N_3O_3$ $[M + H]^+$, 412.2595; found, 412.2591.

N-(3-chlorophenyl)-3-((dimethylamino)methyl)-4-hydroxy-4-(3-methoxyphenyl)-N-methylpiperidine-1-carboxamide hydrochloride (**2e**)

4-nitrophenyl (3-chlorophenyl)(methyl)carbamate (**8e**)

Off-white solid, yield: 99%. ^{1}H NMR (400 MHz, DMSO-d6), δ 8.28 (d, *J* = 8 Hz, 2H), 7.67 (s, 1H), 7.44~7.51 (m, 4H), 7.37 (d, *J* = 8 Hz, 1H), 3.38 (s, 3H). LC-MS-ESI$^+$: $[M + H]^+$ 262.2, $[M + Na]^+$ 284.1.

N-(3-chlorophenyl)-3-((dimethylamino)methyl)-4-hydroxy-4-(3-methoxyphenyl)-N-methylpiperidine-1-carboxamide hydrochloride (**2e**)

Off-white solid, yield: 79%. ^{1}H NMR (400 MHz, CD_3OD), δ 7.24~7.29 (m, 1H), 7.15~7.19 (m, 2H), 7.05 (d, *J* = 4 Hz, 1H), 6.92 (s, 1H), 6.87 (s, *J* = 8 Hz, 1H), 6.89~6.73 (m, 1H), 3.94 (d, *J* = 12 Hz, 1H), 3.66 (s, 3H), 3.37 (d, *J* = 12 Hz, 1H), 3.12 (s, 3H), 2.85~2.99 (m, 3H), 2.51~2.28 (m, 4H), 2.41 (s, 3H), 2.18 (s, 1H), 1.80~1.88 (m, 1H), 1.37 (d, *J* = 16 Hz, 1H), 1.15~1.19 (m, 1H). ^{13}C NMR (150 MHz, CD_3OD) δ 160.55, 159.49, 147.00, 146.50, 134.00, 130.02, 128.87, 123.83, 122.58, 120.89, 116.24, 111.43, 110.44, 72.21, 56.32, 53.70, 43.80, 43.69, 41.78, 40.35, 39.96, 38.12, 37.51. LC-MS-ESI$^+$: $[M + H]^+$ 432.2. HRMS (ESI), calcd for $C_{23}H_{30}ClN_3O_3$ $[M + H]^+$, 432.2048; found, 432.2039.

N-(4-chlorophenyl)-3-((dimethylamino)methyl)-4-hydroxy-4-(3-methoxyphenyl)piperidine-1-carboxamide hydrochloride (**2f**)

Phenyl (4-chlorophenyl)carbamate (**8f**)

Off-white solid, yield: 54%. ^{1}H NMR (400 MHz, $CDCl_3$), δ 7.34~7.45 (m, 4H), 7.23~7.30 (m, 3H), 7.11~7.20 (m, 2H). LC-MS-ESI$^+$: $[M + H]^+$ 248.1, $[M + Na]^+$ 270.1.

N-(4-chlorophenyl)-3-((dimethylamino)methyl)-4-hydroxy-4-(3-methoxyphenyl)piperidine-1-carboxamide hydrochloride (**2f**)

Off-white solid, yield: 91%. ^{1}H NMR (400 MHz, CD_3OD), δ 7.33 (d, *J* = 4 Hz, 2H), 7.18 (t, *J* = 8 Hz, 1H), 7.11 (d, *J* = 4 Hz, 2H), 6.99 (s, 1H), 6.94 (d, *J* = 4 Hz, 1H), 6.72 (dd, *J1* = 8 Hz, *J2* = 4 Hz, 1H), 4.29 (dd, *J1* = 12 Hz, *J2* = 4 Hz, H), 3.93~3.97 (m, 1H), 3.66 (s, 3H), 3.27 (t, *J* = 12 Hz, 1H), 3.08~3.16 (m, 1H), 2.86~2.92 (m, 1H), 2.57~2.60 (m, 4H), 2.4 (s, 3H), 2.25~02.28 (m, 1H), 2.03~2.11 (m, 1H), 1.59 (d, *J* = 8 Hz, 1H). ^{13}C NMR (150 MHz, CD_3OD) δ 159.50, 155.39, 146.65, 137.85, 128.85, 127.45, 126.94, 121.26, 116.38, 111.46, 110.52, 72.42, 56.64, 53.68, 42.99, 40.57, 39.84, 38.47. LC-MS-ESI$^+$: $[M + H]^+$ 418.2. LC-MS-ESI$^-$: $[M + H]^-$ 416.2. HRMS (ESI), calcd for $C_{22}H_{28}ClN_3O_3$ $[M + H]^+$, 419.1923; found, 419.1929.

N-(3,4-dichlorophenyl)-3-((dimethylamino)methyl)-4-hydroxy-4-(3-methoxyphenyl)piperidine-1-carboxamide hydrochloride (**2g**)

Phenyl (3,4-dichlorophenyl)carbamate (**8g**)

Off-white solid, yield: 92.5%. ^{1}H NMR (400 MHz, DMSO-d6), δ 10.57 (s, 1H), 7.80~7.82 (m, 1H), 7.29~7.62 (m, 1H), 7.42~7.49 (m, 3H), 7.24~7.30 (m, 2H). LC-MS-ESI$^+$: $[M+H]^+$ 282.0.

N-(3,4-dichlorophenyl)-3-((dimethylamino)methyl)-4-hydroxy-4-(3-methoxyphenyl)piperidine-1-carboxamide hydrochloride (**2g**)

Off-white solid, yield:82%. ^{1}H NMR (400 MHz, CD_3OD), δ 7.67~7.69 (m, 1H), 7.23~7.29 (m, 2H), 7.16~7.23 (m, 1H), 7.00 (s, 1H), 6.95 (d, *J* = 16 Hz, 1H), 6.72 (d, *J* = 16 Hz, 1H), 4.30 (d, *J* = 12 Hz, 1H), 3.96 (d, *J* = 12 Hz, 1H), 3.67 (s, 3H), 3.28 (t, *J* = 12 Hz, 1H), 2.52~2.61 (m, 7H), 2.26 (m, 1H), 2.04~2.11 (m, 1H), 1.60 (d, *J* = 12 Hz, 1H). ^{13}C NMR (150 MHz, CD_3OD) δ 159.50, 154.89, 146.62, 139.27, 130.95, 129.13, 128.85, 124.44, 120.94, 119.07, 116.40, 111.49, 110.51, 72.41, 56.63, 53.69, 43.09, 40.59, 39.78, 38.45. LC-MS-ESI$^+$: $[M + H]^+$452.2,454.2. LC-MS-ESI$^-$:

$[M + H]^-$450.2, 452.1. HRMS (ESI), calcd for $C_{22}H_{27}Cl_2N_3O_3$ $[M + H]^+$, 452.1502; found, 452.1500.

3-((dimethylamino)methyl)-4-hydroxy-4-(3-methoxyphenyl)-N-(3,4,5-trichlorophenyl)piperidine-1-carboxamide hydrochloride (**2h**)

Phenyl (3,4,5-trichlorophenyl)carbamate (**8h**)

Off-white solid, yield: 71.4%. ^{1}H NMR (400 MHz, $CDCl_3$), δ 7.96~8.00 (m, 2H), 7.42~7.43 (m, 2H), 7.25~7.30 (m, 2H), 7.11~7.15 (m, 1H), 7.02~7.06 (m, 2H), 6.87 (s, 1H). LC-MS-ESI$^+$: $[M + Na]^+$ 338.0, 340.0.

3-((dimethylamino)methyl)-4-hydroxy-4-(3-methoxyphenyl)-N-(3,4,5-trichlorophenyl)piperidine-1-carboxamide hydrochloride (**2h**)

Off-white solid, yield: 81%. ^{1}H NMR (400 MHz, CD_3OD), δ 7.64 (s, 2H), 7.18 (d, *J* = 8 Hz, 1H), 6.99 (s, 1H), 6.94 (d, *J* = 4 Hz, 1H), 6.71 (d, *J* = 4 Hz, 1H), 3.3 (d, *J* = 4 Hz, 1H), 3.96 (dd, *J1* = 16 Hz, *J2* = 4 Hz, 1H), 3.68 (s, 3H), 3.26 (t, *J* = 12 Hz, 1H), 3.10~3.16 (m, 1H), 2.86~2.91 (m, 1H), 2.43~2.60 (m, 7H), 2.23~2.29 (m, 1H), 2.07 (m, *J1* = 12 Hz, *J2* = 4 Hz, 1H), 1.59 (d, *J* = 12 Hz, 1H). ^{13}C NMR (150 MHz, CD_3OD) δ 159.51, 154.52, 146.55, 139.39, 132.57, 128.86, 122.74, 119.14, 116.38, 111.48, 110.51, 72.38, 56.57, 53.68, 42.89, 40.52, 39.92, 38.46. LC-MS-ESI$^+$: $[M + H]^+$ 486.1, 488.1. LC-MS-ESI$^-$: $[M + H]^-$ 484.1, 486.1. HRMS (ESI), calcd for $C_{22}H_{26}Cl_3N_3O_3$ $[M + H]^+$, 486.1113; found, 486.1100.

3-((dimethylamino)methyl)-N-(3-fluorophenyl)-4-hydroxy-4-(3-methoxyphenyl)piperidine-1-carboxamide hydrochloride (**2i**)

Phenyl (3-fluorophenyl)carbamate (**8i**)

Off-white solid, yield: 85%. ^{1}H NMR (400 MHz, $CDCl_3$), δ 7.21~7.28 (m, 3H), 7.08~7.14 (m, 2H), 7.02~7.05 (m, 2H), 6.91~6.95 (m, 2H), 6.62~6.68 (m, 1H). LC-MS-ESI$^+$: $[M + H]^+$ 232.1, $[M + Na]^+$ 254.1.

3-((dimethylamino)methyl)-N-(3-fluorophenyl)-4-hydroxy-4-(3-methoxyphenyl)piperidine-1-carboxamide hydrochloride (**2i**)

Off-white solid, yield: 84%. ^{1}H NMR (400 MHz, CD_3OD), δ 7.265 (d, *J* = 8 Hz, 1H), 7.16~7.20 (m, 1H), 7.09~7.12 (m, 2H), 6.99 (s, 1H), 6.94 (d, *J* = 4 Hz, 1H), 6.72 (dd, *J1* = 8 Hz, *J2* = 4 Hz, 1H), 6.58~6.61 (m, 1H), 4.28~4.31 (m, 1H), 3.94~3.97 (m, 1H), 3.67 (s, 3H), 3.24~3.31 (m, 1H), 3.08~3.17 (m, 1H), 2.86~2.92 (m, 1H), 2.52~2.61 (m, 7H), 2.62 (m, 1H), 2.03~2.11 (m, 1H), 1.57~1.61 (m, 1H). ^{13}C NMR (150 MHz, CD_3OD) δ 162.31 (d, *J* = 241.5 Hz) 159.50, 155.25, 146.63, 141.01, 140.93, 128.85, 128.76, 116.38, 114.94, 111.47, 110.51, 108.14 (d, *J* = 22.5 Hz), 106.46 (d, *J* = 25.5 Hz), 72.42, 56.63, 53.68, 42.88, 40.54, 39.93, 38.49. LC-MS-ESI$^+$: $[M + H]^+$ 402.2. LC-MS-ESI$^-$: $[M + H]^-$ 400.3, $[M + Cl^-]^-$ 436.2. HRMS (ESI), calcd for $C_{22}H_{28}FN_3O_3$ $[M + H]^+$, 402.2187; found, 402.2184.

N-(3,4-difluorophenyl)-3-((dimethylamino)methyl)-4-hydroxy-4-(3-methoxyphenyl)piperidine-1-carboxamide hydrochloride (**2j**)

Phenyl (3,4-difluorophenyl)carbamate (**8j**)

Off-white solid, yield: 87%. ^{1}H NMR (400 MHz, $CDCl_3$), δ 7.32~7.38 (m, 1H), 7.25~7.30 (m, 2H), 7.11~7.17 (m, 1H), 7.03~7.09 (m, 2H), 6.96~7.00 (m, 1H), 6.86~6.93 (m, 2H). LC-MS-ESI$^+$: $[M + H]^+$ 250.1, $[M + Na]^+$ 272.1.

N-(3,4-difluorophenyl)-3-((dimethylamino)methyl)-4-hydroxy-4-(3-methoxyphenyl)piperidine-1-carboxamide hydrochloride (**2j**)

Off-white solid, yield: 81%. ^{1}H NMR (400 MHz, CD_3OD), δ 7.51~7.56 (m, 1H), 7.33 (t, *J* = 8 Hz,

1H), 7.17~7.19 (m, 1H), 7.09 (d, *J* = 8 Hz, 1H), 6.86~6.88 (m, 1H), 4.39~4.43 (m, 1H), 4.05~4.10 (m, 1H), 3.81 (s, 3H), 3.41~3.48 (m, 1H), 3.25 (t, *J* = 12 Hz, 1H), 3.02~3.07 (m, 1H), 2.66~2.75 (m, 7H), 2.39~2.42 (m, 1H), 2.18~2.26 (m, 1H), 1.74 (d, *J* = 8 Hz, 1H). ^{13}C NMR (150 MHz, CD_3OD) δ 159.49, 155.25, 146.64, 136.06, 128.84, 116.36, 115.74 (d, *J* = 18 Hz), 115.56, 111.43, 110.51, 108.95 (d, *J* = 21 Hz), 72.42, 56.62, 53.67, 42.78, 40.57, 39.92, 38.50. LC-MS-ESI$^+$: $[M + H]^+$ 420.3. LC-MS-ESI$^-$: $[M + H]^-$ 418.3, $[M+Cl^-]^-$ 454.3. HRMS (ESI), calcd for $C_{22}H_{27}F_2N_3O_3$ $[M + H]^+$, 420.2093; found, 420.2091.

N-(3-chloro-4-fluorophenyl)-3-((dimethylamino)methyl)-4-hydroxy-4-(3-methoxyphenyl)piperidine-1-carboxamide hydrochloride (**2k**)

Phenyl (3-chloro-4-fluorophenyl)carbamate (**8k**)

Off-white solid, yield: 95.9%. ^{1}H NMR (400 MHz, $CDCl_3$), δ 7.45~7.46 (m, 1H), 7.23~7.30 (m, 2H), 7.06~7.16 (m, 2H), 7.00~7.08 (m, 2H), 6.91~6.99 (m, 1H), 6.82 (s, 1H).

N-(3-chloro-4-fluorophenyl)-3-((dimethylamino)methyl)-4-hydroxy-4-(3-methoxyphenyl)piperidine-1-carboxamide (free base of **2k**)

Off-white solid, yield: 79%. ^{1}H NMR (400 MHz, CD_3OD), δ 7.629 (dd, *J1* = 6.8 Hz, *J2* = 2.8 Hz, 1H), 7.244~7.326 (m, 2H), 7.070~7.122 (t, 2H), 7.026 (d, *J* = 7.6 Hz, 1H), 6.80 (dd, *J1* = 8.4 Hz, *J2* = 2.4 Hz, 1H), 4.307 (dd, *J1* = 13.6 Hz, *J2* = 4 Hz, 1H), 4.036 (d, *J* = 13.6 Hz, 1H), 3.755 (s, 3H), 3.356 (m, *J1* = 13.2 Hz, *J2* = 2.8 Hz, 1H), 3.168~3.230 (t, 1H), 2.803~2.860 (m, 1H), 2.289~2.514 (m, 7H), 2.258~2.309 (m, 1H), 2.137 (m, *J1* = 13.6 Hz, *J2* = 4.8 Hz, 1H), 1.644~1.693 (m, 1H). LC-MS-ESI$^+$: $[M + H]^+$ 436.2; LC-MS-ESI$^-$: $[M-H]^-$ 434.2.

N-(3-chloro-4-fluorophenyl)-3-((dimethylamino)methyl)-4-hydroxy-4-(3-methoxyphenyl)piperidine-1-carboxamide hydrochloride (**2k**)

Off-white solid, yield: 76%. ^{1}H NMR (400 MHz, CD_3OD), δ 7.706 (dd, *J1* = 6.8 Hz, *J2* = 2.8 Hz, 1H), 7.314~7.401 (m, 2H), 7.132~7.184 (m, 2H), 7.097 (d, *J* = 7.6 Hz, 1H), 6.778 (dd, *J1* = 8 Hz, *J2* = 2.4 Hz, 1H), 4.411~4.458 (m, 1H), 4.087 (d, *J* = 6.6 Hz, 1H), 3.819 (s, 3H), 3.403~3.472 (m, 1H), 3.230~3.351 (m, 1H), 3.018~3.075 (m, 1H), 2.720~2.758 (m, 4H), 2.585 (s, 3H), 2.378~2.432 (m, 1H), 2.183~2.262 (m, 1H), 1.719~1.767 (m, 1H). ^{13}C NMR (150 MHz, CD_3OD) δ 159.50, 155.27, 146.61, 136.09, 128.85, 121.75, 119.75, 116.37, 115.23, 115.09, 111.45, 110.51, 72.41, 56.61, 53.68, 42.84, 40.53, 39.89, 38.47. LC-MS-ESI$^+$: $[M + H]^+$ 436.2. LC-MS-ESI$^-$: $[M + H]^-$ 434.2. HRMS (ESI), calcd for $C_{22}H_{27}ClFN_2O_3$ $[M + H]^+$, 436.1798; found, 436.1794.

N-(3,5-bis(trifluoromethyl)phenyl)-3-((dimethylamino)methyl)-4-hydroxy-4-(3-methoxyphenyl)piperidine-1-carboxamide hydrochloride (**2l**)

Phenyl (3,5-bis(trifluoromethyl)phenyl)carbamate (**8l**)

Off-white solid, yield: 85%. ^{1}H NMR (400 MHz, $CDCl_3$), δ 7.96~8.00 (m, 2H), 7.61~7.63 (m, 1H), 7.40~7.46 (m, 2H), 7.26~7.34 (m, 2H), 7.18~7.22 (m, 2H).

N-(3,5-bis(trifluoromethyl)phenyl)-3-((dimethylamino)methyl)-4-hydroxy-4-(3-methoxyphenyl)piperidine-1-carboxamide hydrochloride (**2l**)

Off-white solid, yield: 96.3%. ^{1}H NMR (400 MHz, CD_3OD), δ 8.22 (s, 2H), 7.55 (s, 1H), 7.31~7.35 (m, 1H), 7.10~7.12 (m, 1H), 6.87 (d, *J* = 8 Hz, 1H), 4.51~4.54 (m, 1H), 4.13~4.17 (m, 1H), 3.82 (s, 3H), 3.42~3.49 (m, 1H), 3.28~3.35 (m, 1H), 3.18~3.24 (m, 1H), 3.03~3.08 (m, 1H), 2.74~2.78 (m, 4H), 3.58 (s, 3H), 2.44 (m, 1H), 2.21~2.29 (m, 1H). ^{13}C NMR (150 MHz, CD_3OD) δ 159.50, 154.52, 146.57, 141.57, 130.4 (q, *J* = 33 Hz), 128.86, 123.76, 121.96, 118.71, 116.42, 114.06, 111.53, 110.51, 72.41, 66.10, 56.62, 53.69, 45.88, 43.17, 40.59, 39.74, 38.41, 7.18. LC-MS-ESI$^+$: $[M + H]^+$ 520.3. LC-MS-ESI$^-$: $[M + H]^-$ 518.3; $[M + Cl^-]^-$ 554.3. HRMS (ESI), calcd

for $C_{24}H_{27}F_6N_3O_3$ $[M + H]^+$, 520.2029; found, 520.2017.

3-(3-((dimethylamino)methyl)-4-hydroxy-4-(3-methoxyphenyl)piperidine-1-carboxamido)thiophene-2-carboxylate hydrochloride (**2n**)

Methyl 3-((phenoxycarbonyl)amino)thiophene-2-carboxylate (**8n**)

Off-white solid, yield: 88%. ^{1}H NMR (400 MHz, $CDCl_3$), δ 9.90 (s, 1H), 7.89~7.91 (m, 1H), 7.47~7.52 (m, 1H), 7.39~7.46 (m, 2H), 7.24~7.31 (m, 1H), 7.19~7.23 (m, 2H), 2.93 (s, 3H).

3-(3-((dimethylamino)methyl)-4-hydroxy-4-(3-methoxyphenyl)piperidine-1-carboxamido)thiophene-2-carboxylate hydrochloride (**2n**)

Off-white solid, yield: 90.8%. ^{1}H NMR (400 MHz, CD_3OD), δ 7.77 (d, *J* = 8 Hz, 1H), 7.54 (d, *J* = 8 Hz, 1H), 7.18 (t, *J* = 8 Hz, 1H), 6.99 (s, 1H), 6.94 (d, *J* = 8 Hz, 1H), 7.72 (d, *J* = 8 Hz, 1H), 4.20 (d, *J* = 12 Hz, 1H), 3.85 (d, *J* = 12 Hz, 1H), 3.74 (s, 3H), 3.67 (s, 3H), 3.44 (t, *J* = 12 Hz, 1H), 3.15~3.17 (m, 2H), 2.93~2.99 (m, 1H), 2.59~2.62 (m, 4H), 2.53 (s, 3H), 2.31 (m, 1H), 2.09~2.16 (m, 1H), 1.65 (t, *J* = 12 Hz, 1H). ^{13}C NMR (150 MHz, CD_3OD) δ 164.77, 159.52, 152.98, 146.40, 145.84, 131.31, 128.90, 120.51, 116.35, 111.56, 110.47, 107.31, 72.30, 56.32, 53.69, 50.49, 42.43, 40.21, 38.26. LC-MS-ESI$^+$: $[M + H]^+$ 448.3. HRMS (ESI), calcd for $C_{22}H_{29}N_3O_5S$ $[M + H]^+$, 448.1901; found, 448.1896.

2-(3-((dimethylamino)methyl)-4-hydroxy-4-(3-methoxyphenyl)piperidine-1-carboxamido)thiophene-3-carboxylate hydrochloride (**2o**)

Methyl 2-((phenoxycarbonyl)amino)thiophene-3-carboxylate (**8o**)

Off-white solid, yield: 79%. ^{1}H NMR (400 MHz, $CDCl_3$), δ 10.57 (s, 1H), 7.39~7.43 (m, 2H), 7.19~7.29 (m, 4H), 6.75 (d, *J* = 4 Hz, 1H), 3.91 (s, 3H).

2-(3-((dimethylamino)methyl)-4-hydroxy-4-(3-methoxyphenyl)piperidine-1-carboxamido)thiophene-3-carboxylate hydrochloride (**2o**)

Off-white solid, yield: 97.5%. ^{1}H NMR (400 MHz, CD_3OD), δ 7.19 (t, *J* = 8 Hz, 1H), 7.05 (d, *J* = 4 Hz, 1H), 7.00 (s, 1H), 6.95 (d, *J* = 8 Hz, 1H), 6.73 (d, *J* = 8 Hz, 1H), 6.64 (d, *J* = 8 Hz, 1H), 4.19 (d, *J* = 12 Hz, 1H), 3.80 (d, *J* = 12 Hz, 1H), 3.74 (s, 3H), 3.67 (s, 3H), 3.44~3.47 (m, 1H), 3.19~3.26 (m, 1H), 2.95~3.10 (m, 1H), 2.58~2.63 (m, 7H), 2.33 (m, 1H), 2.11~2.19 (m, 1H), 1.68 (d, *J* = 16 Hz, 1H). ^{13}C NMR (150 MHz, CD_3OD) δ 165.94, 159.53, 152.33, 151.24, 146.31, 128.91, 122.63, 116.36, 114.15, 111.64, 110.44, 110.04, 72.22, 66.10, 56.23, 53.70, 50.24, 42.43, 40.08, 38.13. LC-MS-ESI$^+$: $[M + H]^+$ 448.3. HRMS (ESI), calcd for $C_{22}H_{29}N_3O_5S$ $[M + H]^+$, 448.1901; found, 448.1896.

N-((3s,5s,7s)-adamantan-1-yl)-3-((dimethylamino)methyl)-4-hydroxy-4-(3-methoxyphenyl)piperidine-1-carboxamide hydrochloride (**2p**)

Phenyl ((3s,5s,7s)-adamantan-1-yl)carbamate (**8p**)

Off-white solid, yield: 75%. ^{1}H NMR (400 MHz, $CDCl_3$), δ 7.18~7.25 (m, 2H), 6.96~7.15 (m, 3H), 4.75 (s, 1H), 1.97 (s, 3H), 1.86~1.89 (m, 6H), 1.53~1.58 (m, 6H). LC-MS-ESI$^+$: $[M + H]^+$ 300.2, $[M + Na]^+$ 322.2, $[2M + Na]^+$ 621.4.

N-((3s,5s,7s)-adamantan-1-yl)-3-((dimethylamino)methyl)-4-hydroxy-4-(3-methoxyphenyl)piperidine-1-carboxamide hydrochloride (**2p**)

Off-white solid, yield: 99%. ^{1}H NMR (400 MHz, CD_3OD), δ 7.17~7.22 (m, 1H), 6.90~6.97 (m, 2H), 6.71~6.75 (m, 1H), 4.06 (d, *J* = 12 Hz, 1H), 3.73 (d, *J* = 16 Hz, 1H), 3.67 (s, 3H), 3.07~3.12 (m, 1H), 2.95 (t, *J* = 12 Hz, 1H), 2.83~2.89 (m, 1H), 2.56~2.62 (m, 4H), 2.42 (s, 3H), 2.18 (m, 1H), 1.99~2.04 (m, 1H), 1.94 (s, 9H), 1.59 (s, 6H), 1.54 (d, *J* = 12 Hz, 1H), 1.17 (t, *J* = 8 Hz, 1H). ^{13}C NMR (150 MHz, CD_3OD) δ 159.66, 159.47, 157.08, 146.85, 145.24, 129.16, 128.83, 116.35,

116.13, 112.02, 111.41, 110.49, 110.40, 72.34, 70.60, 56.71, 56.01, 53.77, 53.67, 50.82, 50.65, 45.87, 42.95, 42.52, 41.15, 40.36, 39.70, 39.47, 39.33, 38.28, 37.99, 35.61, 35.09, 34.39, 29.11, 28.38, 7.19. LC-MS-ESI$^+$: $[M + H]^+$ 442.4. HRMS (ESI), calcd for $C_{26}H_{39}N_3O_3$ $[M + H]^+$, 442.3064; found, 442.3060.

N-(1-((3r,5r,7r)-adamantan-1-yl)ethyl)-3-((dimethylamino)methyl)-4-hydroxy-4-(3-methoxyphenyl)piperidine-1-carboxamide hydrochloride (**2q**)

Phenyl (1-((3r,5r,7r)-adamantan-1-yl)ethyl)carbamate (**8q**)

Off-white solid, yield: 93.5%. ^{1}H NMR (400 MHz, $CDCl_3$), δ 7.333~7.394 (m, 2H), 7.128~7.200 (m, 3H), 4.883 (d, *J* = 5 Hz, 1H), 3.436~3.477 (m, 1H), 2.018 (s, 3H), 1.506~1.746 (m, 12H), 1.109~1.158 (m, 3H). LC-MS-ESI$^+$: $[M + H]^+$ 300.2, $[M + Na]^+$ 322.2, $[2M + Na]^+$ 621.4.

N-(1-((3r,5r,7r)-adamantan-1-yl)ethyl)-3-((dimethylamino)methyl)-4-hydroxy-4-(3-methoxyphenyl)piperidine-1-carboxamide(free base of **2q**)

Off-white solid, yield: 24.3%. ^{1}H NMR (400 MHz, CD_3OD), δ 7.28~7.37 (m, 1H), 7.01~7.11 (m, 2H), 6.84~6.87 (m, 1H), 4.18 (d, *J* = 16 Hz,1H), 3.97 (d, *J* = 12 Hz, 1H), 3.80~3.85 (m, 3H), 3.60~3.65 (m, 1H), 3.32~3.39 (m, 1H), 3.09~3.17 (m, 1H), 2.84~2.87 (m, 1H), 2.50~2.59 (m, 7H), 2.24 (m, 1H), 2.09~2.17 (m, 1H), 1.96~2.01 (m, 3H), 1.59~1.76 (m, 14H), 1.08~1.13 (m, 3H). LC-MS-ESI$^+$: $[M + H]^+$ 470.3.

N-(1-((3r,5r,7r)-adamantan-1-yl)ethyl)-3-((dimethylamino)methyl)-4-hydroxy-4-(3-methoxyphenyl)piperidine-1-carboxamide hydrochloride (**2q**)

Off-white solid, yield: 78%. ^{1}H NMR (400 MHz, CD_3OD), δ 7.17(t, *J* = 8 Hz, 1H), 6.94(d, *J* = 4 Hz, 1H), 6.86~6.91(m, 1H), 6.71(dd, *J1* = 8 Hz, *J2* = 4 Hz, 1H), 4.15(d, *J* = 12 Hz, 1H), 3.80 (t, *J* = 16 Hz, 1H), 3.65 (s, 3H), 3.43~3.50 (m, 1H), 3.15~3.23 (m, 1H), 3.00 (t, *J* = 12 Hz, 1H), 2.82~2.91 (m, 1H), 2.53~2.59 (m, 4H), 2.39~2.43 (d, 3H), 2.15~2.17 (m, 1H), 2.01 (m, *J1* = 16 Hz, *J2* = 4 Hz, 1H), 1.84 (d, *J* = 4 Hz, 3H), 1.50~1.62 (m, 7H), 1.45 (s, 6H), 0.94~0.97 (m, 1H). ^{13}C NMR (150 MHz, CD_3OD) δ 159.49, 158.10, 157.97, 146.80, 128.84, 116.30, 116.25, 111.38, 110.52, 72.46, 72.41, 56.61, 56.55, 53.98, 53.86, 53.69, 43.74, 43.69, 43.35, 43.09, 40.44, 40.40, 40.31, 40.08, 39.86, 38.42, 38.38, 37.86, 37.81, 36.59, 36.25, 35.86, 35.74, 35.59, 29.10, 27.93, 27.46, 12.88, 12.67. LC-MS-ESI$^+$: $[M + H]^+$ 470.4. HRMS (ESI), calcd for $C_{28}H_{43}N_3O_3$ $[M + H]^+$, 470.3377; found, 470.3371.

3-((dimethylamino)methyl)-4-hydroxy-N-((1r,3s,5R,7S)-3-hydroxyadamantan-1-yl)-4-(3-methoxyphenyl)piperidine-1-carboxamide hydrochloride (**2r**)

Phenyl ((1r,3s,5R,7S)-3-hydroxyadamantan-1-yl)carbamate (**8r**)

Off-white solid, yield: 87.8%. ^{1}H NMR (400 MHz, $CDCl_3$), δ 7.35 (t, *J* = 8 Hz, 2H), 7.19 (m, *J* = 8 Hz, 1H), 7.11 (d, *J* = 8 Hz, 2H), 4.99 (s, 1H), 2.30 (t, *J* = 4 Hz, 2H), 1.99 (s, 2H), 1.93 (s, 4H), 1.70 (s, 4H), 1.52~1.61 (m, 3H).

3-((dimethylamino)methyl)-4-hydroxy-N-((1r,3s,5R,7S)-3-hydroxyadamantan-1-yl)-4-(3-methoxyphenyl)piperidine-1-carboxamide hydrochloride (**2r**)

Off-white solid, yield: 94%. ^{1}H NMR (400 MHz, CD_3OD), δ 7.19 (d, *J* = 8 Hz, 1H), 6.91~9.74 (m, 1H), 6.71~6.74 (m, 1H), 4.07 (d, *J* = 16 Hz, 1H), 3.75 (d, *J* = 12 Hz, 1H), 3.67 (s, 3H), 3.06~3.14 (m, 2H), 2.96 (t, *J* = 12 Hz, 1H), 2.83~2.88 (m, 1H), 2.56~2.62 (m, 4H), 2.42 (s, 3H), 2.18 (m, 1H), 2.10 (s, 2H), 1.96~2.04 (m, 1H), 1.79~1.89 (m, 6H), 1.41~1.55 (m, 8H), 1.16~1.19 (m, 1H). ^{13}C NMR (150 MHz, CD_3OD) δ 159.47, 157.04, 146.83, 128.83, 116.35, 111.40, 110.50, 72.34, 67.83, 56.72, 53.68, 53.15, 48.19, 45.88, 42.99, 42.86, 40.37, 39.91, 39.78, 38.28, 34.23, 30.17, 7.18. LC-MS-ESI$^+$: $[M + H]^+$ 458.4. LC-MS-ESI$^-$: $[M + Cl^-]^-$492.4. HRMS (ESI), calcd for

$C_{26}H_{39}N_3O_4$ $[M + H]^+$, 458.3013; found, 458.3004.

3-((dimethylamino)methyl)-4-hydroxy-4-(3-hydroxyphenyl)-N-phenylpiperidine-1-carboxamide (**11**)

Foam-like solid, yield: 60%. ^{1}H NMR (400 MHz, CD3OD), δ 7.39 (d, *J* = 8 Hz, 2H), 7.27 (t, *J* = 8 Hz, 2H), 7.16 (t, *J* = 8 Hz, 2H), 7.02 (t, *J* = 8 Hz, 1H), 6.93 (d, *J* = 8 Hz, 2H), 6.66 (d, *J* = 8 Hz, 2H), 4.15 (dd, *J1* = 12 Hz, *J2* = 4 Hz, 2H), 3.22~3.34 (m, 3H), 2.27~2.33 (q, 1H), 2.02~2.08 (m, 9H), 1.93 (d, *J* = 16 Hz, 1H), 1.66 (d, *J* = 16 Hz, 1H).

3-((dimethylamino)methyl)-4-hydroxy-4-(3-hydroxyphenyl)-N-phenylpiperidine-1-carboxamide hydrochloride (**12**)

Off-white solid, yield: 94%. ^{1}H NMR (400 MHz, CD_3OD), δ 7.44 (d, *J* = 8 Hz, 2H), 7.28 (d, *J* = 8 Hz, 2H), 7.23 (d, *J* = 8 Hz, 1H), 7.04 (d, *J* = 8 Hz, 1H), 6.985 (d, *J* = 4 Hz, 2H), 6.71~6.73 (m, 1H), 4.38~4.42 (m, 1H), 4.07~4.11 (m, 1H), 3.44 (t, *J* = 12 Hz, 1H), 3.22~3.34 (m, 2H), 3.01~3.07 (q, 1H), 2.76~2.79 (m, 4H), 2.59 (s, 3H), 2.34 (m, 1H), 2.21 (m, *J1* = 12 Hz, *J2* = 4 Hz, 1H), 1.75 (d, *J* = 16 Hz, 1H). ^{13}C NMR (150 MHz, CD_3OD) δ 159.00, 157.93, 148.69, 140.88, 130.90, 129.82, 129.66, 124.32, 122.28, 117.29, 115.28, 113.47, 74.39, 58.70, 45.78, 44.92, 42.66, 42.13, 40.46. HRMS (ESI), calcd for $C_{21}H_{27}N_3O_3$ $[M + Na]^+$, 392.1945; found, 392.1936.

Pharmacology

Receptor binding assay

Cell membrane preparation followed the reported procedure[57]. Ligand competition binding experiments used [^{3}H]DAMGO (50.1 Ci/mmol) for rat μ opioid receptor, [^{3}H]DPDPE (52.7 Ci/mmol) for rat δ opioid receptor, [^{3}H]U69593 (39.1 Ci/mmol) for human κ opioid receptor, respectively. Binding assay was conducted in 50 mM Tris-HCl buffer solution (pH 7.4) at 37 °C for 30 min in triplicate in a final volume of 0.5 ml with 30 μg of membrane protein. Nonspecific binding employed U50488H, DAMGO, or DPDPE at a concentration of 10 μM. Radio ligand bound membrane protein was separated by fast filtration via GF/B filter paper under reduce pressure. Then the radioactivity of filter paper was dried under oven and was determined by liquid scintillation counting. Binding data and K_i values were calculated using GraphPad Prism 6.0 program.

[^{35}S]GTPγS Binding assay

[^{35}S]GTPγS binding assay was performed according to procedure reported before[56]. Membranes (15 μg/sample) were incubated with 0.1 nM [^{35}S]GTPγS (1030 Ci/mmol, PerkinElmer) in a binding buffer consisting of 50 mM Tris-HCl, pH 7.4, 1 mM EDTA, 5 mM $MgCl_2$, 100 mM NaCl, and 40 μM GDP at 30 °C for 1 h in the presence of increasing concentrations of compounds. Nonspecific binding was determined in the presence of nonradioactive GRPγS (10 μM). Incubations were terminated by rapid filtration, and bound radioactivity was determined by liquid scintillation counting. The percentage of stimulated [^{35}S]GTPγS binding was calculated according to formula: $100\times(cpm_{sample}-cpm_{nonspecific})/(cpm_{basal}-cpm_{nonspecific})$. EC_{50} and E_{max} were analyzed and calculated with GraphPad prism 6.0 program.

Animals

Kunming strain female mice (18 ~ 22 g) were obtained from the Animal Holding Unit, School of Pharmacy of Fudan University. Mice were housed in groups (6 mice/group) and raised in an environment of 12 h light/dark cycle in a constant temperature (20 ~ 26 ^{0}C). Mice were free access to food and sterilized water. All animal experiments were conducted under the guidelines of the National Institutes of Health Guide for the Care and Use of Laboratory Animals using an

approved animal protocol.

Hot plate antinociception test.

The hot plate test conducted according to reported procedure[58]. Hot plate was maintained for 55.0 ^{0}C for mice. Before dosing a drug, animal was placed on the smooth hot plate surface to test its latency threshold defined as time interval after animal was put on the heated surface to licking back paws and a cutoff time of 30 seconds was maintained to prevent from mice injury. Mice with latency threshold of 5~30 s were selected to further dosing. Latency was measured twice before dosing and mean value was defined as basal latency. After dosing of drugs, latency threshold was tested and a cutoff time of 60 seconds was maintained to prevent mice injury. Antinociception was calculated by the following formula: maximum possible effect (MPE)%=100× (test latency–basal latency)/ (cutoff time–basal latency). ED_{50} (dose of drug that produce 50% MPE) were determined using a computer-assisted linear analysis of the dose-response curve. Antagonism effect was conducted by dosing naloxone after 10 min before drug injection.

Molecular modeling

Homology modeling

Active homo sapiens MOR (sequence NO.: P35372) was built from murine active MOR (PDB NO.: 5C1M, resolution: 2.1 Å) as template using Discovery Studio 3.5. Sequence identity and sequence similarity of both receptors were 97.3%, 98.3%, respectively. Active homo sapiens DOR (sequence NO.: P41143) was built from homo sapiens active KOR (PDB NO.: 6B73, resolution: 3.1 Å) as template using Discovery Studio 3.5. Sequence identity and sequence similarity of both receptors were 93.9%, 98.1%, respectively. Ramachandran plot of active homo sapiens MOR and DOR were shown below. Homo sapiens KOR (PDB NO.: 6B73, resolution: 3.1 Å) was employed.

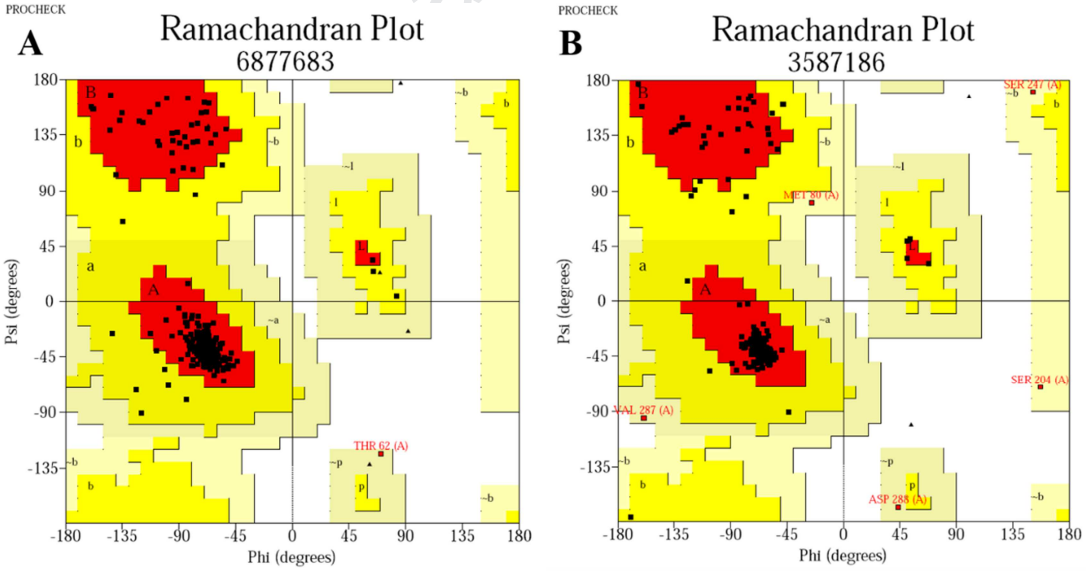

Ramachandran plot of Active homo sapiens MOR and DOR (**A**: MOR, optimum region 95.2%, acceptance region 99.6%; **B**: DOR, optimum region 93.9%, acceptance region 98.1%))

Docking and plotting

Docking studies were performed in induce-fitting module of Schrödinger 3.5. Pymol 0.99 was employed in plotting.

Acknowledgement

This work is supported by grants from National Natural Science Foundation of China (NO. 81773635) and Shanghai Science and Technology Development Funds (14431900500).

Conflict of interest

The authors declared no conflict of interest.

Reference

[1] H. Schmidhammer,M. Spetea, Development of 5-Substituted N-Methylmorphinan-6-ones as Potent Opioid Analgesics with Improved Side-Effect Profile, International Journal of Medicinal Chemistry 2012 (2012) 1-10.

[2] A. Dahan, Respiratory Depression with Opioids, Journal Of Pain & Palliative Care Pharmacotherapy 21 (2007) 63-66.

[3] A. Dahan, L. Aarts,T.W. Smith, Incidence, Reversal, and Prevention of Opioid-induced Respiratory Depression, Anesthesiology 112 (2010) 226-238.

[4] E. Freye,L. Latasch, Development of opioid tolerance -- molecular mechanisms and clinical consequences, Anasthesiol Intensivmed Notfallmed Schmerzther 38 (2003) 14-26.

[5] A.D. Kaye, M.R. Jones, A.M. Kaye, J.G. Ripoll, V. Galan, B.D. Beakley, F. Calixto, J.L. Bolden, R.D. Urman,L. Manchikanti, Prescription Opioid Abuse in Chronic Pain: An Updated Review of Opioid Abuse Predictors and Strategies to Curb Opioid Abuse: Part 1, Pain Physician 20 (2017) S93-S109.

[6] L.R. Webster, Opioid-Induced Constipation, Pain Med. 16 (2015) S16-S21.

[7] H.S. Smith,A. Laufer, Opioid induced nausea and vomiting, Eur. J. Pharmacol. 722 (2014) 67-78.

[8] L.H. Chen, H. Hedegaard,M. Warner, Drug-poisoning Deaths Involving Opioid Analgesics: United States, 1999-2011, NCHS Data Brief (2014) 1-8.

[9] A. Kolodny, D.T. Courtwright, C.S. Hwang, P. Kreiner, J.L. Eadie, T.W. Clark,G.C. Alexander, The Prescription Opioid and Heroin Crisis: A Public Health Approach to an Epidemic of Addiction, Annu. Rev. Publ. Health 36 (2015) 559-574.

[10] H. Jalal, J.M. Buchanich, M.S. Roberts, L.C. Balmert, K. Zhang,D.S. Burke, Changing dynamics of the drug overdose epidemic in the United States from 1979 through 2016, Science 361 (2018) u1184.

[11] K. Simpson, P. Leyendecker, M. Hopp, S. Müller-Lissner, O. Löwenstein, J. De Andrés, J. Troy Ferrarons, B. Bosse, B. Krain, T. Nichols, W. Kremers,K. Reimer, Fixed-ratio combination oxycodone/naloxone compared with oxycodone alone for the relief of opioid-induced constipation in moderate-to-severe noncancer pain, Curr. Med. Res. Opin. 24 (2008) 3503-3512.

[12] L. Nelson,R. Schwaner, Transdermal fentanyl: pharmacology and toxicology, J Med Toxicol 5 (2009) 230-241.

[13] B. Nicholson, Benefits of Extended-Release Opioid Analgesic Formulations in the Treatment of Chronic Pain, Pain Pract. 9 (2009) 71-81.

[14] B. Jordan,L.A. Devi, Molecular mechanisms of opioid receptor signal transduction, Brit. J. Anaesth. 81 (1998) 12-19.

[15] R.S. Duman, J.F. Tallman,E.J. Nestler, Acute and chronic opiate-regulation of adenylate cyclase in brain: specific effects in locus coeruleus, The Journal of pharmacology and experimental therapeutics 246 (1988) 1033.

[16] S.D.M.L. Andrea M. Trescot, Opioid Pharmacology, Pain Physician 11 (2008) S133-S153.

[17] R.R.G.F. Laura M. Bohn, μ-Opioid receptor desensitization by β-arrestin-2 determines morphine tolerance but not dependence, Nature 408 (2000) 720-723.

[18] K.M. Raehal, Morphine Side Effects in β-Arrestin 2 Knockout Mice, J. Pharmacol. Exp. Ther. 314 (2005) 1195-1201.

[19] M. Connor, E.E. Bagley, B.C. Chieng,M.J. Christie, β-Arrestin-2 knockout prevents development of cellular μ-opioid receptor tolerance but does not affect opioid-withdrawal-related adaptations in single PAG neurons, Brit. J. Pharmacol. 172 (2015) 492-500.

[20] C.L. Schmid, N.M. Kennedy, N.C. Ross, K.M. Lovell, Z. Yue, J. Morgenweck, M.D. Cameron, T.D. Bannister,L.M. Bohn, Bias Factor and Therapeutic Window Correlate to Predict Safer Opioid Analgesics, Cell 171 (2017) 1165-1175.

[21] R.J.L.R. Laura M. Bohn, Enhanced Morphine Analgesia in Mice Lacking β-Arrestin 2, Science 286 (1999) 2495-2498.

[22] X. Chen, P. Pitis, G. Liu, C. Yuan, D. Gotchev, C.L. Cowan, D.H. Rominger, M. Koblish, S.M. DeWire, A.L. Crombie, J.D. Violin,D.S. Yamashita, Structure–Activity Relationships and Discovery of a G Protein Biased μ Opioid Receptor Ligand, [(3-Methoxythiophen-2-yl)methyl]({2-[(9R)-9-(pyridin-2-yl)-6-oxaspiro-[4.5]decan-9-yl]ethyl})amine (TRV130), for the Treatment of Acute Severe Pain, J. Med. Chem. 56 (2013) 8019-8031.

[23] S.M. DeWire, D.S. Yamashita, D.H. Rominger, G. Liu, C.L. Cowan, T.M. Graczyk, X.T. Chen, P.M. Pitis, D. Gotchev, C. Yuan, M. Koblish, M.W. Lark,J.D. Violin, A G Protein-Biased Ligand at the μ-Opioid Receptor Is Potently Analgesic with Reduced Gastrointestinal and Respiratory Dysfunction Compared with Morphine, J. Pharmacol. Exp. Ther. 344 (2013) 708-717.

[24] D.G. Soergel, R.A. Subach, N. Burnham, M.W. Lark, I.E. James, B.M. Sadler, F. Skobieranda, J.D. Violin,L.R. Webster, Biased agonism of the μ-opioid receptor by TRV130 increases analgesia and reduces on-target adverse effects versus morphine: A randomized, double-blind, placebo-controlled, crossover study in healthy volunteers, Pain 155 (2014) 1829-1835.

[25] E.R. Viscusi, L. Webster, M. Kuss, S. Daniels, J.A. Bolognese, S. Zuckerman, D.G. Soergel, R.A. Subach, E. Cook,F. Skobieranda, A randomized, phase 2 study investigating TRV130, a biased ligand of the μ-opioid receptor, for the intravenous treatment of acute pain, Pain 157 (2016) 264-272.

[26] N. Singla, H. Minkowitz, D. Soergel, D. Burt, R.A. Subach, M. Salamea, M. Fossler,F. Skobieranda, A randomized, Phase IIb study investigating oliceridine (TRV130), a novel μ-receptor G-protein pathway selective (μ-GPS) modulator, for the management of moderate to severe acute pain following abdominoplasty, Journal of Pain Research 10 (2017) 2413-2424.

[27] C. Austin Zamarripa, S.R. Edwards, H.N. Qureshi, J.N. Yi, B.E. Blough,K.B. Freeman, The G-protein biased mu-opioid agonist, TRV130, produces reinforcing and antinociceptive effects that are comparable to oxycodone in rats, Drug Alcohol Depen. 192 (2018) 158-162.

[28] S. Dogra,P.N. Yadav, Biased agonism at kappa opioid receptors: Implication in pain and mood disorders, Eur. J. Pharmacol. 763 (2015) 184-190.

[29] L.M. Bohn,J. Aubé, Seeking (and Finding) Biased Ligands of the Kappa Opioid Receptor, ACS Med. Chem. Lett. 8 (2017) 694-700.

[30] L. Zhou, K.M. Lovell, K.J. Frankowski, S.R. Slauson, A.M. Phillips, J.M. Streicher, E. Stahl, C.L. Schmid, P. Hodder, F. Madoux, M.D. Cameron, T.E. Prisinzano, J. Aubé,L.M. Bohn, Development of Functionally Selective, Small Molecule Agonists at Kappa Opioid Receptors, J. Biol. Chem. 288 (2013) 36703-36716.

[31] K.L. White, J.E. Robinson, H. Zhu, J.F. DiBerto, P.R. Polepally, J.K. Zjawiony, D.E. Nichols, C.J.

Malanga,B.L. Roth, The G Protein-Biased -Opioid Receptor Agonist RB-64 Is Analgesic with a Unique Spectrum of Activities In Vivo, J. Pharmacol. Exp. Ther. 352 (2014) 98-109.

[32] K.M. Lovell, K.J. Frankowski, E.L. Stahl, S.R. Slauson, E. Yoo, T.E. Prisinzano, J. Aubé,L.M. Bohn, Structure‐Activity Relationship Studies of Functionally Selective Kappa Opioid Receptor Agonists that Modulate ERK 1/2 Phosphorylation While Preserving G Protein Over βArrestin2 Signaling Bias, ACS Chem. Neurosci. 6 (2015) 1411-1419.

[33] E.L. Maillet, N. Milon, M.D. Heghinian, J. Fishback, S.C. Schürer, N. Garamszegi,D.C. Mash, Noribogaine is a G-protein biased κ-opioid receptor agonist, Neuropharmacology 99 (2015) 675-688.

[34] K.L. White, J.E. Robinson, H. Zhu, J.F. DiBerto, P.R. Polepally, J.K. Zjawiony, D.E. Nichols, C.J. Malanga,B.L. Roth, The G Protein-Biased κ-Opioid Receptor Agonist RB-64 Is Analgesic with a Unique Spectrum of Activities In Vivo, J. Pharmacol. Exp. Ther. 352 (2015) 98-109.

[35] T.F. Brust, J. Morgenweck, S.A. Kim, J.H. Rose, J.L. Locke, C.L. Schmid, L. Zhou, E.L. Stahl, M.D. Cameron, S.M. Scarry, J. Aubé, S.R. Jones, T.J. Martin,L.M. Bohn, Biased agonists of the kappa opioid receptor suppress pain and itch without causing sedation or dysphoria, Sci. Signal. 9 (2016) a117.

[36] Z. Zheng, X. Huang, T.J. Mangano, R. Zou, X. Chen, S.A. Zaidi, B.L. Roth, R.C. Stevens,V. Katritch, Structure-Based Discovery of New Antagonist and Biased Agonist Chemotypes for the Kappa Opioid Receptor, J. Med. Chem. 60 (2017) 3070-3081.

[37] A.S. Yekkirala, D.P. Roberson, B.P. Bean,C.J. Woolf, Breaking barriers to novel analgesic drug development, Nat. Rev. Drug Discov. 16 (2017) 545-564.

[38] M.E. Olson, L.M. Eubanks,K.D. Janda, Chemical Interventions for the Opioid Crisis: Key Advances and Remaining Challenges, J. Am. Chem. Soc. 141 (2019) 1798-1806.

[39] Q. Shen, Y. Qian, X. Xu, W. Li, J. Liu,W. Fu, Design, synthesis and biological evaluation of N-phenylalkyl-substituted tramadol derivatives as novel μ opioid receptor ligands, Acta Pharmacol. Sin. 36 (2015) 887-894.

[40] Q. Shen, Y. Qian, X. Huang, X. Xu, W. Li, J. Liu,W. Fu, Discovery of Potent and Selective Agonists of δ Opioid Receptor by Revisiting the "Message-Address" Concept, ACS Med. Chem. Lett. 7 (2016) 391-396.

[41] https://www.drugs.com/dosage/tramadol.html.

[42] R. Schwyzer, ACTH: a short introductory review, Ann N Y Acad Sci 297 (1977) 3-26.

[43] P.S. Portoghese, Bivalent ligands and the message-address concept in the design of selective opioid receptor antagonists, Trends Pharmacol. Sci. 10 (1989) 230-235.

[44] P.S. Portoghese, M. Sultana,A.E. Takemori, Design of peptidomimetic delta opioid receptor antagonists using the message-address concept, J. Med. Chem. 33 (1990) 1714-1720.

[45] G. Dondio, S. Ronzoni, D.S. Eggleston, M. Artico, P. Petrillo, G. Petrone, L. Visentin, C. Farina, V. Vecchietti,G.D. Clarke, Discovery of a novel class of substituted pyrrolooctahydroisoquinolines as potent and selective delta opioid agonists, based on an extension of the message-address concept, J. Med. Chem. 40 (1997) 3192-3198.

[46] J.R. Healy, P. Bezawada, N.W. Griggs, A.L. Devereaux, R.R. Matsumoto, J.R. Traynor, A. Coop,C.W. Cunningham, Benzylideneoxymorphone: A new lead for development of bifunctional mu/delta opioid receptor ligands, Bioorg. Med. Chem. Lett. 27 (2017) 666-669.

[47] S. Ananthan, N.K. Khare, S.K. Saini, L.E. Seitz, J.L. Bartlett, P. Davis, C.M. Dersch, F. Porreca, R.B. Rothman,E.J. Bilsky, Identification of Opioid Ligands Possessing Mixed μ Agonist/δ

Antagonist Activity among Pyridomorphinans Derived from Naloxone, Oxymorphone, and Hydropmorphone, J. Med. Chem. 47 (2004) 1400-1412.

[48] R. Hron,B.S. Jursic, Preparation of substituted semicarbazides from corresponding amines and hydrazines via phenyl carbamates, Tetrahedron Lett. 55 (2014) 1540-1543.

[49] A.W. Bannon,A.B. Malmberg, Models of Nociception: Hot‐Plate, Tail‐Flick, and Formalin Tests in Rodents, Current Protocols in Neuroscience 41 (2007).

[50] C. Gillen, M. Haurand, D.J. Kobelt,S. Wnendt, Affinity, potency and efficacy of tramadol and its metabolites at the cloned human μ-opioid receptor, Naunyn-Schmiedeberg's Archives of Pharmacology 362 (2000) 116-121.

[51] W. Huang, A. Manglik, A.J. Venkatakrishnan, T. Laeremans, E.N. Feinberg, A.L. Sanborn, H.E. Kato, K.E. Livingston, T.S. Thorsen, R.C. Kling, S. Granier, P. Gmeiner, S.M. Husbands, J.R. Traynor, W.I. Weis, J. Steyaert, R.O. Dror,B.K. Kobilka, Structural insights into μ-opioid receptor activation, Nature 524 (2015) 315-321.

[52] A. Koehl, H. Hu, S. Maeda, Y. Zhang, Q. Qu, J.M. Paggi, N.R. Latorraca, D. Hilger, R. Dawson, H. Matile, G.F.X. Schertler, S. Granier, W.I. Weis, R.O. Dror, A. Manglik, G. Skiniotis,B.K. Kobilka, Structure of the μ-opioid receptor–Gi protein complex, Nature 558 (2018) 547-552.

[53] T. Che, S. Majumdar, S.A. Zaidi, P. Ondachi, J.D. McCorvy, S. Wang, P.D. Mosier, R. Uprety, E. Vardy, B.E. Krumm, G.W. Han, M. Lee, E. Pardon, J. Steyaert, X. Huang, R.T. Strachan, A.R. Tribo, G.W. Pasternak, F.I. Carroll, R.C. Stevens, V. Cherezov, V. Katritch, D. Wacker,B.L. Roth, Structure of the Nanobody-Stabilized Active State of the Kappa Opioid Receptor, Cell 172 (2018) 55-67.

[54] T. Claff, J. Yu, V. Blais, N. Patel, C. Martin, L. Wu, G.W. Han, B.J. Holleran, O. Van der Poorten, K.L. White, M.A. Hanson, P. Sarret, L. Gendron, V. Cherezov, V. Katritch, S. Ballet, Z.J. Liu, C.E. Muller,R.C. Stevens, Elucidating the active delta-opioid receptor crystal structure with peptide and small-molecule agonists, Sci Adv 5 (2019) x9115.

[55] R.B. Raffa, E. Friderichs, W. Reimann, R.P. Shank, E.E. Codd,J.L. Vaught, Opioid and nonopioid components independently contribute to the mechanism of action of tramadol, an 'atypical' opioid analgesic, The Journal of pharmacology and experimental therapeutics 260 (1992) 275-285.

[56] R.B. Raffa, E. Friderichs, W. Reimann, R.P. Shank, E.E. Codd, J.L. Vaught, H.I. Jacoby,N. Selve, Complementary and synergistic antinociceptive interaction between the enantiomers of tramadol, The Journal of pharmacology and experimental therapeutics 267 (1993) 331-340.

[57] L. Xiao, Y. Wang, M. Zhang, W. Wu, L. Kong, Y. Ma, X. Xu, X. Liu, Q. He, Y. Qian, H. Sun, H. Wu, C. Lin, H. Huang, R. Ye, S. Jiang, R. Ye, C. Yuan, S. Fang, D. Xue, X. Yang, H. Chen, Y. Zheng, L. Yu, Q. Xie, L. Zheng, W. Fu, W. Li, Z. Qiu, J. Liu,L. Shao, Discovery of a Highly Selective and Potent κ Opioid Receptor Agonist from N-Cyclopropylmethyl-7α-phenyl-6,14-endoethanotetrahydronorthebaines with Reduced Central Nervous System (CNS) Side Effects Navigated by the Message–Address Concept, J. Med. Chem. (2019).

[58] Y. Wang, Y. Tao, F. Li, Y. Wang, X. Xu, J. Chen, Y. Cao, Z. Chi, J.L. Neumeyer, A. Zhang,J. Liu, Pharmacological Characterization of ATPM [(-)-3-Aminothiazolo[5,4-b]-N-cyclopropylmethylmorphinan hydrochloride], a Novel Mixed κ-Agonist and μ-Agonist/-Antagonist That Attenuates Morphine Antinociceptive Tolerance and Heroin Self-Administration Behavior, J. Pharmacol. Exp. Ther. 329 (2009) 306-313.

Discovery of 3-((dimethylamino)methyl)-4-hydroxy-4-(3-methoxyphenyl)-N-phenylpiperidine-1-carboxamide as Novel Potent Analgesic

Huoming Huang [a], Wenli Wang [a], Xuejun Xu [b], Chen Zhu [a], Yujun Wang [b], Jinggen Liu [b*], Wei Li [a*], Wei Fu [a*]

Affiliation:

a. Department of Medicinal Chemistry, School of Pharmacy, Fudan University, Shanghai, 201203, China.

b. Shanghai Institute of Materia Medica, Chinese Academy of Science, Shanghai, 201203, China.

Highlights

1. A series of 3-((dimethylamino)methyl)-4-hydroxy-4-(3-methoxyphenyl)piperidine-1-carboxamide derivatives were designed based on “Address-message concept”.
2. *In vitro* and *in vivo* evaluation afforded compound **2a** as potent analgesic.
3. Compound **2a** was potent in hot plate model (ED_{50} = 3.1 mg/kg).
4. Antinociception of compound **2a** was blocked by naloxone.
5. Binding mode of compound **2a** was proposed.

Discovery of

3-((dimethylamino)methyl)-4-hydroxy-4-(3-methoxyphenyl)-N-phenylpiperidine-1-carboxamide as Novel Potent Analgesic

Huoming Huang [a], Wenli Wang [a], Xuejun Xu [b], Chen Zhu [a], Yujun Wang [b], Jinggen Liu [b*], Wei Li [a*], Wei Fu [a*]

Affiliation:

a. Department of Medicinal Chemistry, School of Pharmacy, Fudan University, Shanghai, 201203, China.

b. Shanghai Institute of Materia Medica, Chinese Academy of Science, Shanghai, 201203, China.

Conflict of interest

The authors declare that they have no known competing financial interests or personal relationships that could have appeared to influence the work reported in this paper.